

Distinct transcriptional signatures in purified circulating immune cells drive heterogeneity in disease location in IBD

Bram Verstockt ,^{1,2} Sare Verstockt ,¹ Jonathan Cremer,¹ João Sabino,^{1,2} Marc Ferrante,^{1,2} Severine Vermeire,^{1,2} Padhmanand Sudhakar ¹

To cite: Verstockt B, Verstockt S, Cremer J, *et al.* Distinct transcriptional signatures in purified circulating immune cells drive heterogeneity in disease location in IBD. *BMJ Open Gastro* 2023;**10**:e001003. doi:10.1136/bmjgast-2022-001003

► Additional supplemental material is published online only. To view, please visit the journal online (<http://dx.doi.org/10.1136/bmjgast-2022-001003>).

Received 5 August 2022
Accepted 25 October 2022



© Author(s) (or their employer(s)) 2023. Re-use permitted under CC BY. Published by BMJ.

¹KU Leuven Department of Chronic Diseases, Metabolism and Ageing, Translational Research Center for Gastrointestinal Disorders (TARGID), IBD group, KU Leuven, Leuven, Belgium

²Department of Gastroenterology and Hepatology, University Hospitals Leuven, Leuven, Belgium

Correspondence to

Dr Padhmanand Sudhakar; padhmanand.sudhakar@kuleuven.be

ABSTRACT

Objective To infer potential mechanisms driving disease subtypes among patients with inflammatory bowel disease (IBD), we profiled the transcriptome of purified circulating monocytes and CD4 T-cells.

Design RNA extracted from purified monocytes and CD4 T-cells derived from the peripheral blood of 125 endoscopically active patients with IBD was sequenced using Illumina HiSeq 4000NGS. We used complementary supervised and unsupervised analytical methods to infer gene expression signatures associated with demographic/clinical features. Expression differences and specificity were validated by comparison with publicly available single cell datasets, tissue-specific expression and meta-analyses. Drug target information, druggability and adverse reaction records were used to prioritise disease subtype-specific therapeutic targets.

Results Unsupervised/supervised methods identified significant differences in the expression profiles of CD4 T-cells between patients with ileal Crohn's disease (CD) and ulcerative colitis (UC). Following a pathway-based classification (Area Under Receiver Operating Characteristic - AUROC=86%) between ileal-CD and UC patients, we identified MAPK and FOXO pathways to be downregulated in UC. Coexpression module/regulatory network analysis using systems-biology approaches revealed mediatory core transcription factors. We independently confirmed that a subset of the disease location-associated signature is characterised by T-cell-specific and location-specific expression. Integration of drug-target information resulted in the discovery of several new (*BCL6*, *GPR183*, *TNFAIP3*) and repurposable drug targets (*TUBB2A*, *PRKCCQ*) for ileal CD as well as novel targets (*NAPEPLD*, *SLC35A1*) for UC.

Conclusions Transcriptomic profiling of circulating CD4 T-cells in patients with IBD demonstrated marked molecular differences between the IBD-spectrum extremities (UC and predominantly ileal CD, sandwiching colonic CD), which could help in prioritising particular drug targets for IBD subtypes.

INTRODUCTION

Inflammatory bowel disease (IBD) is a complex disease of the gut, characterised by chronic intestinal inflammation and resulting in reduction in quality-of-life indices.¹ Besides a complex and multifactorial disease

WHAT IS ALREADY KNOWN ON THIS TOPIC

⇒ Inflammatory bowel disease (IBD) patients with different disease location phenotypes exhibit molecular differences at the primary disease site resulting in varying therapeutic responses.

WHAT THIS STUDY ADDS

⇒ Using gene-expression profiles from the blood-derived immune cells of a wide-spectrum of patients with IBD differing by disease location, we identified a core signature segregating ileal Crohn's disease and UC patients, partly supported by validation at the tissue-level. By integrating drug target and druggability data, we also identified disease location-based subtype specific therapeutic targets.

HOW THIS STUDY MIGHT AFFECT RESEARCH, PRACTICE OR POLICY

⇒ Tailored therapies targeting specific subtypes of IBD could help clinicians to overcome the existing therapeutic ceiling prevalent in IBD treatments.

pathogenesis,² IBD incorporates a wide spectrum of clinical phenotypes.³ The binary split of IBD into Crohn's disease (CD) and ulcerative colitis (UC) is primarily based on the macroscopic and microscopic involvement of the gastrointestinal (GI) tract, while CD is characterised by the presence of transmural, but discontinuous inflammation along the entire GI tract, UC is marked by the occurrence of continuous inflammation spreading from the anal margin and is confined to the colonic mucosa.⁴ Additional phenotypical characterisation is primarily based on the Montreal classification, which has limitations and is purely clinical.⁴ Based on emerging evidence, IBD is more and more perceived as a continuous spectrum with UC and ileal CD at both edges of the spectrum.⁴

At a molecular and cellular level, various differences among ileal CD, colonic CD and UC have been revealed: aggregated genetic risk scores representing the cumulative burden of mutations in known IBD risk loci

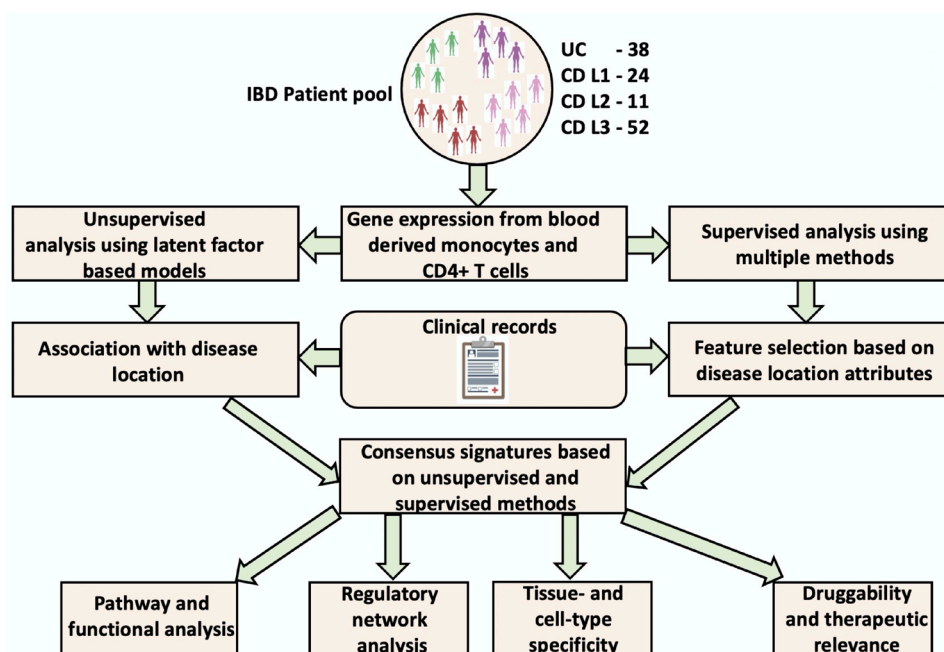


Figure 1 Figurative representation of the workflow used in the study. Unsupervised analysis was carried out using the Multi Omic Factor Analysis (MOFA) tool while the supervised arm of the analysis was executed using DIABLO, netDx, DeSeq2 and BioNERO. Pathway and regulatory network analyses was performed using the ReactomePA package and ChEA3 resource respectively. Tissue-/cell-type specificity and druggability analyses were carried out using publicly available resources such as Human Protein Atlas and OpenTargets/DGIdb/TARDIS respectively. More detailed explanations on the tools used can be found in the Glossary section as well as the methods section of the manuscript. DIABLO, Data Integration Analysis for Biomarker discovery using Latent variable approaches for Omics; DGIdb, Drug-Gene Interaction Database; IBD, inflammatory bowel disease; TARDIS, Target-Adverse Reaction Database Integrated Search.

did introduce the concept of a disease spectrum along the disease location axis.⁵ Also, ileal CD is characterised by a distinct T-cell profile comprising Th1 and Th17 cellular subtypes, while colonic CD is more marked by the Th1 profile.⁶

Purified immune cells from the blood of patients with IBD have previously been used to clinically characterise patients in terms of prognosis⁷ and drug response.⁸ Recent studies have pointed to a significant degree of concordance (between peripheral whole blood and colonic tissue in paediatric patients with IBD.⁹ In addition, blood-based biomarkers have been identified and suggested as surrogate markers of mucosal healing and endoscopic response in Ulcerative colitis^{10 11} as well as predictors of anti-TNF α non-response in IBD.¹² CD4 T-cells and monocyte-derived macrophages not only play a critical role in mediating disease pathogenesis at the primary disease site(s), but also are known to be altered with respect to their activity in the blood circulatory system.^{13–15} In this study, we use gene expression measurements from circulating monocytes and CD4 T-cells, purified from whole blood, to unravel some molecular differences between patients with IBD with various disease locations. Using a combination of supervised and unsupervised approaches (figure 1), we inferred genes, their modules and regulators which could potentially contribute to the differences observed along the IBD spectrum.

METHODS

Patient selection

This study was conducted at the University Hospitals Leuven (Leuven, Belgium). Blood was collected from 125 consecutive patients with IBD (24 CD L1, 11 CD L2, 52 CD L3, 38 UC, based on Montreal classification) with endoscopy-proven active disease (presence of ulcerations in case of CD; Mayo endoscopic subscore 2–3 for UC) (online supplemental table 1)

RNA sequencing and preprocessing of transcriptomic datasets

Cell separation, fluorescence activated cell sorting, and isolation of RNA were performed as reported earlier.¹⁶ TruSeq Stranded mRNA protocol (Illumina, San Diego, USA) according to the manufacturer's instructions was used for the library preparation. Illumina HiSeq 4000NGS was then used for the next-generation single-end sequencing. Alignment of the raw reads from the RNA-sequencing to the reference genome was performed using Hisat2 V.2.1.0.¹⁷ Absolute counts were subsequently generated using HTSeq.¹⁸ Only genes with at least 10 reads in at least 70% of the samples were considered. The remaining datasets were subsequently normalised using the varianceStabilizingTransformation function of the daMiRseq R package. A within-sample filtering based on correlation (≥ 0.85) was used to detect and exclude outliers.



Multiomic factor analysis

Multiomic factor analysis (MOFA)¹⁹ was used to identify the contributions of the individual transcriptomic datasets to the overall variance. The top 5000 features as ranked by the mean absolute deviation from each of the two datasets were used as the input for building the MOFA model. Clinical confounder variables such as age, gender, exposure to previous therapies, steroid, immunomodulator and/or biological use were regressed out. DropFactorThreshold was set at 2% in order to reflect the selection of latent factors capturing at least 2% variance. Model finetuning was performed by evaluating the performance of 100 random initialisations. The model with the highest evidence lower bound was selected as the best one for further implementation. Latent factors representing at least 5% variance in any one of the datasets were considered as significant and were used for further analyses. The top 1000 features corresponding to the latent factors contributing at least 5% variance were retrieved. Two-tailed Student's t-test was used to infer relationships among continuous variables.

Weighted gene coexpression network analysis

A variance filter was applied to select the top 5000 genes from the count filtered normalised dataset. The gene coexpression network was inferred using BioNERO.²⁰ Parameters such as the soft threshold was optimised by testing the fitness of the inferred coexpression network to the scale-free topology. Network type was set to unsigned. Module stability was assessed by performing resampling runs (n=30) and assessing the conservation of the modules after every sampling run. The relevance of the modules to the phenotypes (as determined by the association of the module eigengenes to the traits) was assessed to be significant at FDR (False Discovery Rate) ≤ 0.1 . Gene–gene relationships from the phenotypically relevant modules were further filtered by setting the gene–gene Pearson correlation coefficient threshold at 0.6. Hubs were identified by using a combination of two metrics namely module membership and connectivity. Hub genes were defined as the top 10% of the genes with the highest degree which have a module membership of greater than 0.8.

Differential expression analysis

Pairwise differential expression analysis was carried out using DeSeq2²¹ on the normalised datasets for the different combinations based on disease location. Genes with an absolute log2 fold change of ≥ 1 and an adjusted p ≤ 0.1 were considered to be differentially expressed.

Data Integration Analysis for Biomarker discovery using Latent variable approaches for Omics

For the Data Integration Analysis for Biomarker discovery using Latent variable approaches for Omics (DIABLO)²² analysis, the hyperparameter of the design matrix was set at 0.1. The optimal number of components was determined by performing a M-fold validation with 5 folds and

100 repeats. The number of components to be tested for the optimisation run was set at 10. The optimal number of components was selected based on the weighted votes of the various distance measures and error rates. Similarly, the optimal number of features per-omic dataset for each of the components (from the previous step) was determined by running a M-fold validation with 5 folds and 100 repeats. The final model was executed based on the optimised number of components and the number of features per block per component.

netDx

netDx²³ was used to build a pathway-based classifier with the input being the normalised gene expression datasets labelled with the corresponding phenotypes. The classifier was built using a set value of 100 for the number of iterations. Maximum feature score was set at 10 with a minimum feature selection score threshold set at 9. Training data were assigned as 70% of the corresponding starting dataset. Only features which passed the minimum feature selection score threshold for at least 90% of the iterations were considered as significant. The aggregated signalling pathways (http://download.baderlab.org/EM_Genesets/March_01_2021/Human/, version March 2021) was used as the feature source to project the gene expression data.

Functional enrichment analysis

The ReactomePA²⁴ and clusterProfiler²⁵ R packages were used to check for the presence of over-represented Reactome signalling pathways. Correction for multiple testing was performed with the Benjamini-Hochberg method. Reactome pathways with an FDR ≤ 0.1 were deemed significant. Functional terms with ≤ 10 entities were discarded from the analysis.

Regulatory network reconstruction

Transcriptional regulatory networks driving the expression of the phenotypically relevant coexpression modules were reconstructed by integrating the edges within the respective modules with ChIP-seq and independent coexpression datasets from high-throughput measurements. ChIP-seq and independent coexpression relationships corresponding to the two phenotypically relevant gene modules identified using WGCNA²⁶ were retrieved from ChEA3,²⁷ which is an orthogonal evidence-based resource to identify regulatory and gene–gene relationships. From within the ChEA3 resource, ChIP-seq datasets were retrieved from the parent sources (ENCODE,²⁸ ReMap²⁹ and literature) whereas additional coexpression data were downloaded from GTEx³⁰ and ARCHS4.³¹ An edge (gene–gene relationship) from the phenotypically relevant coexpression module was annotated as a regulatory relationship if one of the genes of the edge is a transcription factor capable of binding to the cis-regulatory elements of the other gene comprising the edge. In addition, if the genes corresponding to the above inferred regulatory relationship were identified

as being coexpressed based on independent inferences as recorded in the GTEx and ARCHS4 databases, then the regulatory relationship was annotated with this extra information which could enhance the probability of it being a true regulatory interaction.

Tissue-type and cell-type origins

Tissue-type and cell-type specific information was retrieved from the Human Protein Atlas.³² Single cell transcriptomic datasets were confined to those genes, which were annotated to be ‘group-enriched’, ‘cell-type enriched’ or ‘cell-type enhanced’. As for blood cell specificity in terms of gene expression, genes ‘not detected in immune cells’ or having ‘low immune cell specificity’ were discarded. Similarly, for RNA blood lineage specificity in terms of gene expression, genes ‘not detected’ in blood cells or having ‘low lineage specificity’ were discarded. Single cell transcriptomic and RNA blood lineage specificity datasets corresponding to the category of ‘T-cells’ were retrieved while those of the available and relevant T-cell subtypes (‘memory CD4 T-cells’, ‘naive CD4 T-cells’ and ‘Tregs’) were used in case of blood cell specific gene expression. Gene expression differences between UC patients and non-IBD controls were retrieved from a previously published meta-analysis using eight different datasets.³³

Disease and therapeutic relevance

Drug targets used in IBD, and other IMIDs such as rheumatoid arthritis (RA), primary sclerosing cholangitis (PSC), ankylosing spondylitis (AS) and psoriasis (PS) were derived from OpenTargets,³⁴ whereas IBD relevant genes corresponding to barrier function,³⁵ antimicrobial peptides,³⁶ cell-adhesion molecules³⁷ and IBD susceptibility loci³⁸ were retrieved from the corresponding literature sources. IBD eQTLs were retrieved from Di Narzo *et al.*³⁹ Druggability information was retrieved from Drug–Gene Interaction Database (DGIdb),⁴⁰ while adverse drug reaction records corresponding to drug targets were obtained from the Target-Adverse Reaction Database Integrated Search platform which stores integrated records collected from various individual databases such as Drug Target Commons,⁴¹ STITCH,⁴² FAERS FDA Adverse Event Reporting System,⁴³ MedEffect,⁴⁴ Side Effect Resource⁴⁵ and Offsides.⁴⁶ Expression signature-based screening against drug induced expression libraries were performed against the LINCS database.⁴⁷

RESULTS

Unsupervised analysis identifies prominent drivers and pathways of IBD pathogenesis

Before harnessing supervised approaches, we used MOFA, an unsupervised methodology, to infer genes with highly variant expression patterns. Unsupervised analysis aids in the identification of these underlying patterns in a large dataset, which subsequently can be investigated for their association with relevant clinical phenotypes. Results from the unsupervised integration of the two

gene-expression datasets (figure 2A, online supplemental figure 1) pointed to two (LF1, LF2) latent factors, (analogous to components of a principal component analysis, PCA) which capture at least 5% variance from both the datasets. For each of the two cell types, comparative analysis of the features as ranked by the weights of the LFs indicated the presence of unique cell-type specific signatures in each LF. Based on the weights (used to rank the features) which are representative of the variance in expression levels, the top-features identified in each of the two cell-types (online supplemental tables 2–6, online supplemental figure 1) capture key drivers in the monocytes and CD4 T-cells of patients with IBD. Among those are *IL1B*, *CD69*, *OSM*, *GOS2*, *IL8*, *CD83* in monocytes, which all have established roles in IBD pathophysiology and/or intestinal inflammation. Similarly, top hits in the CD4 T-cell dataset including *NR4A2*, *SLC2A3*, *SMAD7*, *TFNAIP3*, *RGS1* have previously been reported in the context of IBD (table 1, online supplemental tables 2–6, online supplemental figure 1).

Subsequently, we investigated the association between LFs and enrichment of clinical variables. Only LF2 displayed a significant association ($R^2=0.28$, FDR=0.012) with disease location, but did not correlate with any other clinically relevant variables (disease duration, CRP) tested, indicating its specificity with respect to disease location. Although sample clustering based on the weights assigned by LF2 did not result in a perfect segregation based on disease location status (along the phenotypic axis of L1, L2, L3, UC), we observed a significant difference ($p=0.003$) in the scores assigned by LF2 to L1 and UC samples (figure 2B).

Orthogonal supervised approaches recapitulate consensus signatures captured by the strongest latent factors and segregate UC and CD ileal subtypes

To complement our observations from the unsupervised approach, we performed supervised analysis using three independent tools (DeSeq2, DIABLO and netDx), which aids the inference of consensus signatures inferred by more than any single tool or method and hence enriching the interpretations. Irrespective of the tool used and in line with the unsupervised analysis, we could identify signatures in CD4 T-cells (figure 2C), which segregated UC from CD L1 individuals (and not comparisons between other combination of samples differing by disease location) through circulating CD4 T cell transcriptomics. To further characterise the signatures from each tool, we compared the functional content in terms of the over-represented signalling pathways (figure 2D). In addition, we also performed a coexpression network analysis (online supplemental figure 2) to confirm the inferences made using the three above-mentioned supervised tools.

While DeSeq2 produced the most conservative signature in the form of differentially expressed genes (DEGs) between L1 and UC (online supplemental figure 3), the CD4 T cell signature set from DIABLO (online

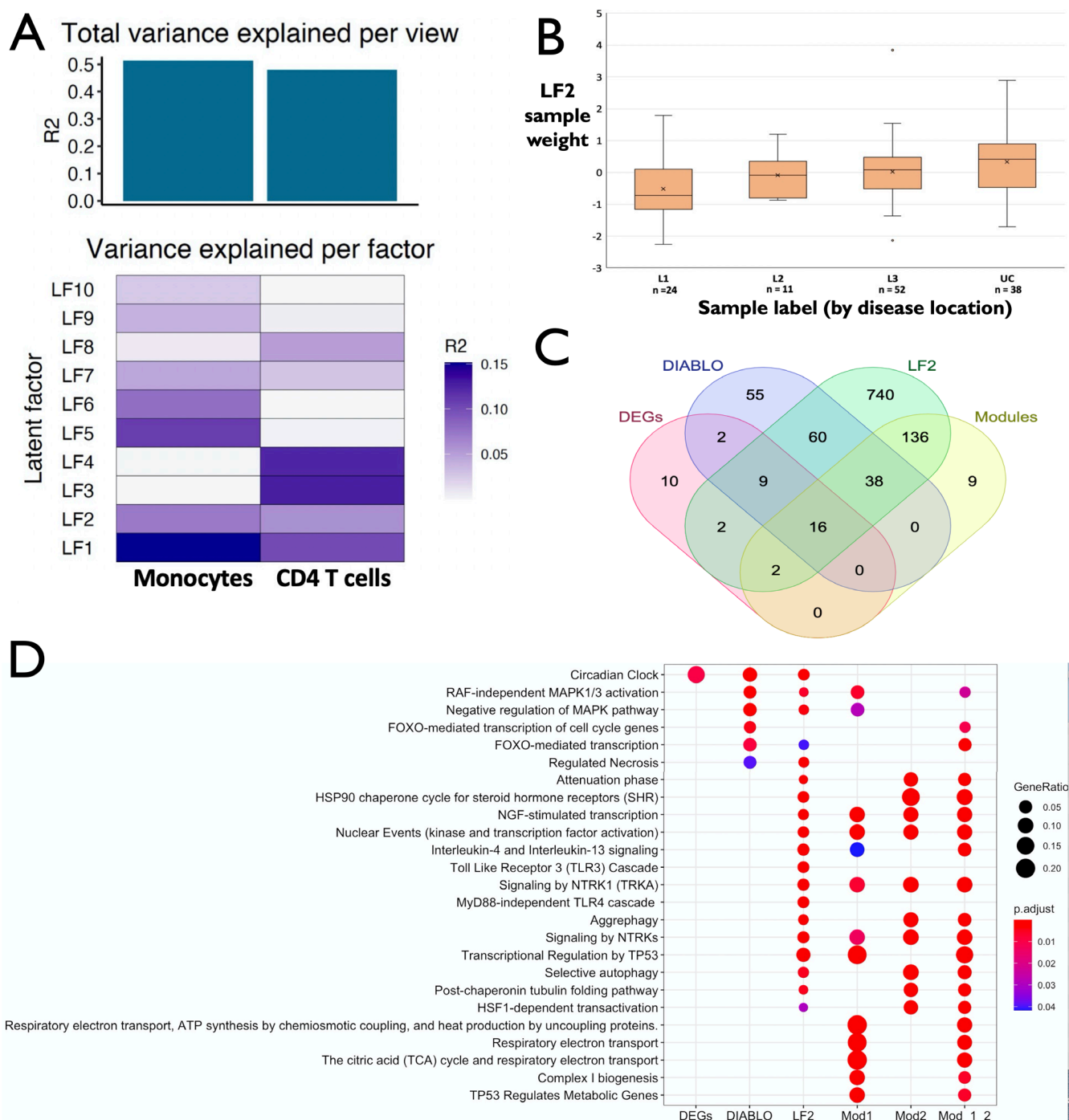


Figure 2 (A) Fraction of total variance explained by the individual latent factors per dataset and proportion of total variance captured cumulatively by the CD4 and monocyte gene-expression datasets. (B) Weights assigned by LF2 to disease location/ diagnosis segregated samples. (C) Overlap among the CD4 T cell derived gene expression signatures distinguishing UC and ileal CD patients, inferred from multiple supervised and unsupervised approaches. LF2, Latent factor 2 (associated with disease location) as inferred by MOFA; Modules: union of the two gene coexpression modules associated with disease location. (D) Comparison of over-represented pathways within signature gene sets segregating UC and ileal CD gene expression in CD4 T-cells. Mod_1_2: Union sum of the modules 1 and 2 associated with the disease location-based phenotypic axis segregating UC and ileal CD patients. CD, Crohn's disease; DEGs, differentially expressed genes; DIABLO, Data Integration Analysis for Biomarker discovery using Latent variable approaches for Omics studies; UC, ulcerative colitis.

supplemental figure 4), the strongest latent factor from MOFA (LF2) as well as the two phenotypically relevant coexpression modules (online supplemental figures 2, 5) were enriched with multiple pathways. Some including

the RAF-independent MAPK-activation pathway and FOXO-mediated transcriptional pathway (figure 3A–C, online supplemental figure 6) were over-represented in multiple signature sets derived from different



Table 1 Top ranking features of the monocytes CD4 T cell gene expression dataset as weighted by the latent factor LF2 which is associated with disease location

Gene symbol	Latent factor (dataset)	Encoded protein	IBD relevant function	Reference
NR4A2	LF2 (CD4 T cells)	Nuclear receptor subfamily 4 group A member 2	Imparts protection against IBD by silencing TRAF6/TLR-IL-1R signalling	72
CSRNP1	LF2 (CD4 T cells)	Cysteine/serine-rich nuclear protein 1	–	–
SLK1	LF2 (CD4 T cells)	Serine/threonine-protein kinase SIK1	Identified as a possible drug target for colitis based on small-molecule screening	73
FOSB	LF2 (CD4 T cells)	Protein fosB	–	–
NR4A1	LF2 (CD4 T cells)	Nuclear receptor subfamily 4 group A member 1	Susceptibility loci in a Japanese family with CD; Modulation of inflammation-associated intestinal fibrosis	74 75
NR4A3	LF2 (monocytes)	Nuclear receptor subfamily 4 group A member 3	–	–
IL1B	LF2 (monocytes)	Interleukin-1 beta	Increases intestinal tight junction permeability	76 77
CD69	LF2 (monocytes)	Early activation antigen CD69	Modulates mucosal inflammation in patients with IBD	78
PDE4B	LF2 (monocytes)	cAMP-specific 3',5'-cyclic phosphodiesterase 4B	PDE4 Inhibition confers protection against UC	79
OSM	LF2 (monocytes)	Oncostatin-M	Drives intestinal inflammation and predicts response to tumour necrosis factor-neutralising therapy; Mediates STAT3-dependent intestinal epithelial restitution; Predicts Crohn's disease response to Infliximab; Biomarker of poor biochemical response to Infliximab	80–84

Only the top five features are shown along with their roles in IBD pathogenesis and/or intestinal inflammation. CD, Crohn's disease; IBD, inflammatory bowel disease; UC, ulcerative colitis.

approaches. Pathway-level classification using the netDx classifier resulted in an AUROC of 86% (online supplemental figures 7, 8) between ileal CD and UC patients. The features which drive the segregation between the two patient groups include pathways such as FOXO-mediated signalling, p38(MAPK)-mediated signalling among others.

To further unravel the blood-derived signals associated with disease location, we investigated their cell and tissue specificity. About 16% of the genes within the disease location-based CD4 T-cell signature (with available single cell transcriptomic data) are expressed in T-cells (figure 3D, online supplemental figure 9). Meanwhile, the equivalent measure for blood-derived T-cells was determined to be about 33%, pointing to a certain level of cell-type specificity of our disease location-associated CD4 T-cell signature segregating ileal CD and UC patients. However, only a small fraction (4.2%) of the genes in CD4 T-cell signature could be traced to intestinal origins based on their expression.

Regulatory networks driving CD4 T cell gene expression signatures reveal a core set of master transcription factors

To infer the control mechanisms which drive the expression of phenotypically relevant genes, we used experimentally verified transcriptional regulatory and coexpression networks. The correlational nature of coexpression networks and the mechanistic knowledge imparted by transcriptional interactions enables the

integration of contextual signals with the underlying cis-regulatory wiring. As a first step, we detected highly inter-connected gene sets representing groups of genes with similar expression patterns (online supplemental figures 2, 5). Of the 14 modules detected, only 2 were significantly associated ($FDR \leq 0.1$) with disease location. Functional enrichment analysis of the modules not only revealed genes corresponding to prominent pathways such as the MAPK pathway and IL-4/IL-13 signalling, for example, in module 1, but also of various modulators and accessory molecules (such as CDKN1A (figure 3E), which influences the activity of the MAPK pathway). More than two-thirds (9/13) of the enriched pathways in module 1 were unique to module 1 compared with module 2. Enriched pathways common to both the modules include those related to NTRK signalling and NGF-stimulated transcription (figure 2D). Top hubs of the coexpression network include *PPP1R15A*, *TUBA1A*, *CSRNP1*, *FOSB* and *ZFP36* in module 1 and *TUBB4B*, *SERTAD1*, *FAM53C*, *PLK2* and *HEXIM1* in module 2.

Since gene coexpression networks representing gene-gene relationships were shown to capture context specificity, we used the phenotypically relevant coexpression modules to further infer the underlying mechanistic interactions such as regulatory relationships by annotating the module edges with ChIP-seq data derived from high-throughput experiments and independent coexpression measurements. Seventy-five per cent (55/73) of

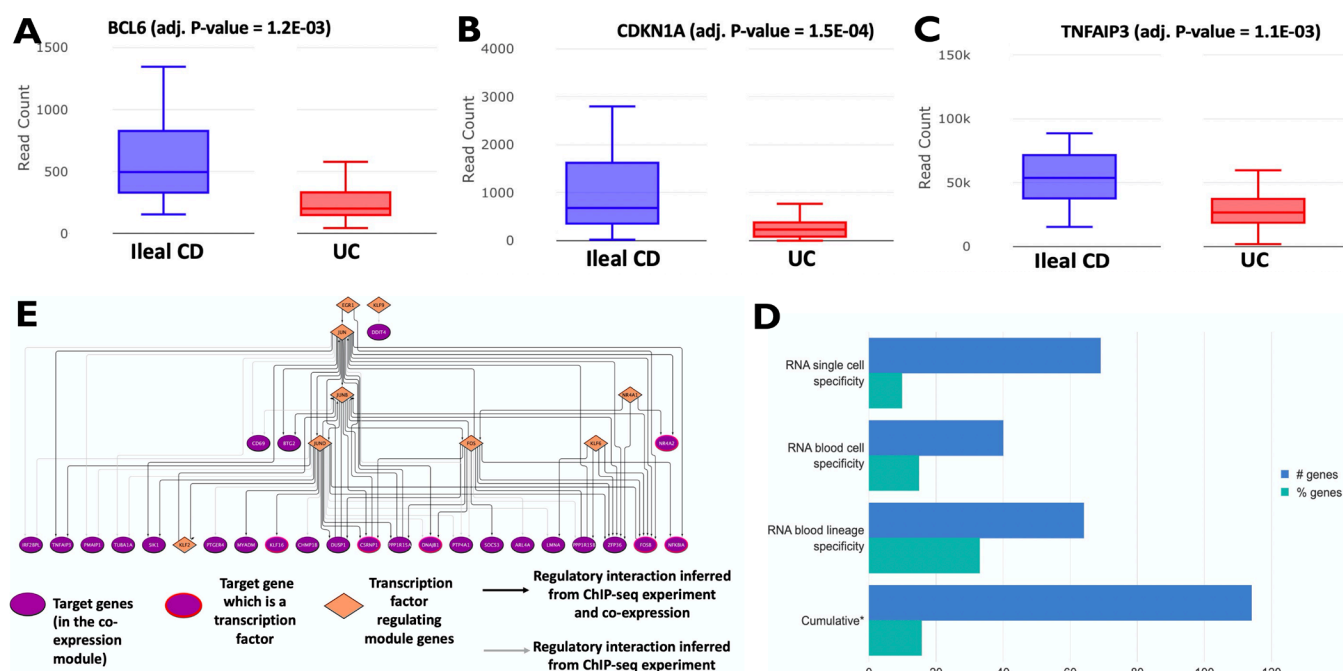


Figure 3 (A, B) Difference in the transcriptional expression between ileal CD and UC patients of FOXO-pathway members *BCL6* and *CDKN1A*. (C) Difference in the transcriptional expression between ileal CD and UC patients of *TNFAIP3*. (D) Summary of cell-type specific expression profiles for the disease location (ileal CD vs UC) associated signature. Using publicly available gene expression datasets at the level of single cells and beyond from the Human Protein Atlas (HPA), we inferred the cell-type specificity of the disease location-associated genes. Essentially, the figure represents the overlap between the disease location (ileal CD vs UC) associated genes in CD4 T cells and (D) Genes expressed in various T-cell populations as inferred by RNA sequencing at the resolution of single cells (RNA single cell specificity) irrespective of sample source, genes expressed in various blood-derived T-cell populations (RNA blood cell specificity), genes expressed in blood-derived T-cell populations at the level of cell-lineages (RNA blood lineage specificity). (*) The cumulative number is the non-redundant sum of all of the above categories. The numbers are represented both as a fraction and absolute gene count of all the disease location-associated genes. Please refer to the Methods section for more details on the filtering procedure used. (E) Transcriptional regulatory network modulating the expression of the coexpression module 1 associated with disease location. CD, Crohn's disease; UC, ulcerative colitis.

the edges within the coexpression module 1 associated with disease location were characterised by regulatory binding, as well as independent coexpression relationships (figure 3E). Nodes within the coexpression module 1 encoded for biologically relevant proteins such as *SOCS3*, *NFKB1A*, *TNFAIP3* (figure 3A–C) among others. Furthermore, this coexpression module was regulated by multiple core transcription factors of the JUN family, *FOS*, *NR4A1*, *EGR1* and three TFs (*KLF2*, *KLF6*, *KLF9*) from the Krueppel-like factor family of transcription factors. The abovementioned TFs also regulated various other transcription factors such as *NR4A2*, *NFKB1*, *KLF16*, *DNAJB1* and *CSRNP1*, all found within the same coexpression module. Despite its low connectivity, *EGR1* acts as a master regulator by modulating the expression of upstream transcription factors such as *JUN*. Module 2 on the other hand was characterised by a sparse regulatory network with a low number of inferred interactions (data not shown).

Therapeutic and disease relevance of immune-cell-derived molecular targets associated with disease location

Functional relevance of the inferred signatures is essential for biological interpretation and shortlisting targets for therapeutic interventions. We; therefore, compared the genes (and/or their expression) making up our disease location-associated signature with (A) previously identified IBD-relevant genes, (B) targets of drugs used in IBD and other IMIDs and (C) by exploring the druggability and adverse reactions of hitherto unexplored targets. For the above analysis, we used the set of genes which were identified by at least two methods (from among MOFA, DEGs, DIABLO and coexpression analysis).

To substantiate the functional importance of the two phenotypically relevant CD4 T cell signature associated with disease location, the signature genes were matched against pre-existing gene sets corresponding to IBD drug targets,³⁴ IBD relevant genes (barrier function,³⁵ antimicrobial peptides,³⁶ cell-adhesion molecules,³⁷ IBD susceptibility loci,³⁸ literature search) and IBD eQTLs³⁹ (figure 4A). About 23% (61/265) of the disease location-associated signature genes were linked to IBD pathogenesis (online supplemental table 6) and 28/61 were also

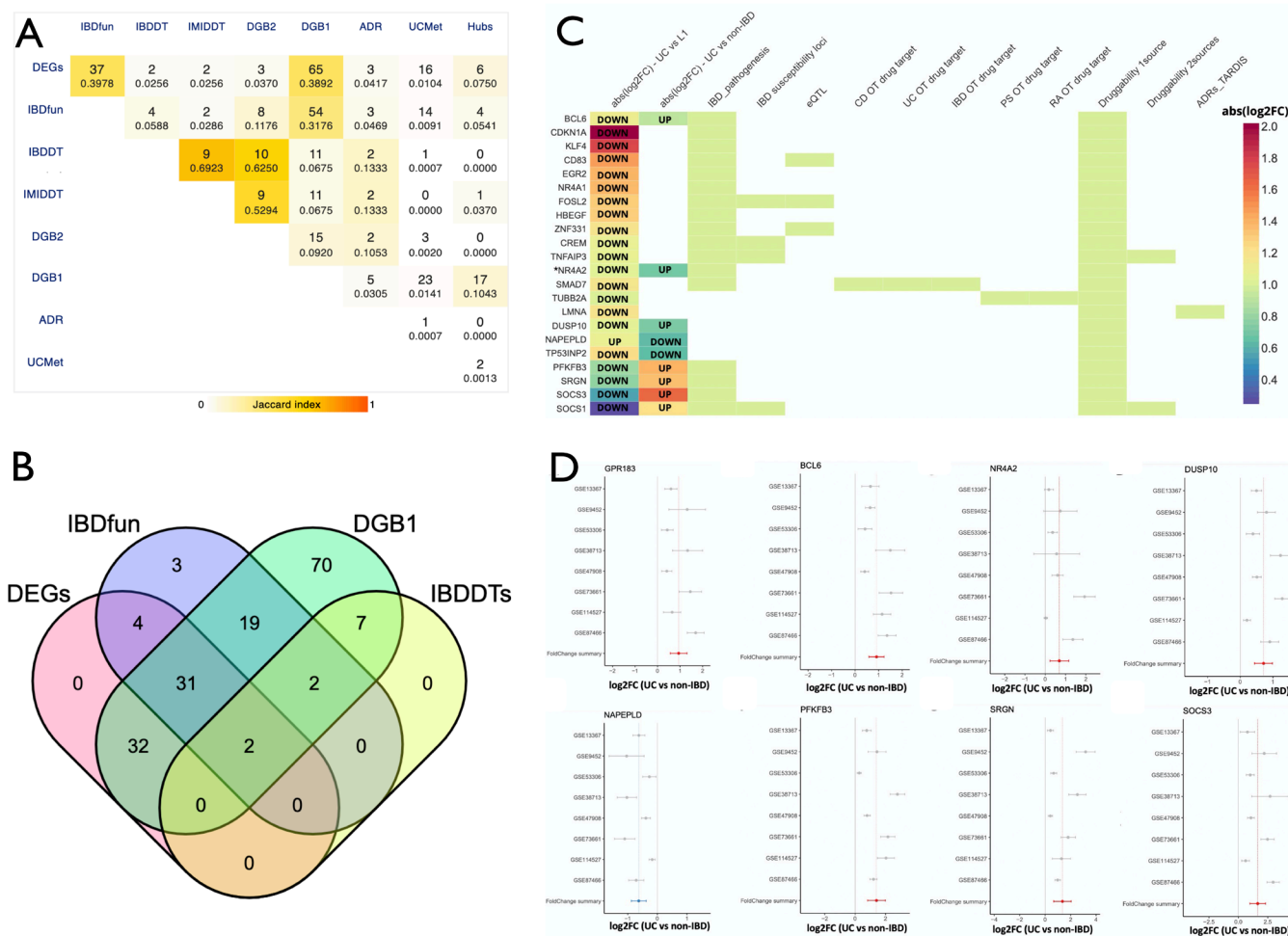


Figure 4 (A) Correlation matrix representing the overlap profile (of the disease location associated signature) between the gene categories involved in IBD pathogenesis (IBDfun), therapeutically targeted in IBD (IBDDTs), in IMIDs (IMIDDTs), those identified as druggable targets (DGB1 and DGB2 for targets assigned as druggable by DGIdb based on one and two sources, respectively) and those with adverse drug reactions (ADR). DEGs: differentially expressed genes (UC vs L1) at log2 fold change ≥ 0.5 and at an adjusted $p \leq 0.1$; UCMeta: genes differentially expressed (as identified by a meta-analysis) in the intestinal mucosa between UC and non-IBD controls. (B) Disease location signature genes distributed with respect to their role in IBD pathogenesis (IBDfun), status in terms of being therapeutically targeted in IBD (IBDDTs), druggability (DGB1) and differential expression (log2 fold change ≥ 0.5 and adjusted $p \leq 0.1$) between UC vs L1 patients. (C) IBD pathogenesis and therapeutic relevance of the CD4 T cell signature (differentiating ileal CD and UC patients) associated with disease location. abs (log2FC) – UC vs L1: absolute fold change difference of gene expression between UC and ileal CD patients; abs (log2FC) – UC vs non-IBD: absolute fold change difference of gene expression between UC patients and non-IBD controls as inferred from a meta-analysis³³; AMP genes: genes encoding anti-microbial peptides; IBD susceptibility loci: susceptibility genes identified by³⁸; eQTL: expression based Quantitative Trait Loci (QTL) retrieved from Di Narzo *et al.*³⁹ CD OT drug target: drug targets used in Crohn's disease as identified from the OpenTargets database³⁴; UC OT drug target: drug targets used in Ulcerative colitis as identified from the OpenTargets database³⁴; IBD OT drug target: drug targets used in IBD as identified from the OpenTargets database³⁴; PS OT drug target: drug targets used in psoriasis disease as identified from the OpenTargets database³⁴; RA OT drug target: drug targets used in RA disease as identified from the OpenTargets database³⁴; Druggability—2 sources: targets identified as 'druggable' by at least two sources in the Drug Gene Interaction database DGIdb⁴⁰; Druggability—1 sources: targets identified as 'druggable' by at least one source in the Drug Gene Interaction database DGIdb⁴⁰; ADR record: information as recorded in Target-Adverse Reaction Database Integrated Search (TARDIS). Genes with evidence from each of above-mentioned classes were filtered based on the absolute log2 fold change ≥ 1 in one of the two expression datasets (UC vs L1 OR UC vs non-IBD) and sorted; *annotation of the genes in terms of their identification as a hub in the coexpression modules associated with disease location. (D) Expression differences between UC patients and non-IBD controls (based on the results of a meta-analysis) for some of the candidate disease location associated genes with therapeutic potential. ADR, adverse drug reaction; CD, Crohn's disease; IBD, inflammatory bowel disease; RA, rheumatoid arthritis; UC, ulcerative colitis.

annotated as eQTLs. In total, only 4 (*CXCR4*, *PRKCQ*, *PTGER4* and *SMAD7*) of the 57 disease location-associated genes relevant to IBD pathogenesis were known to be

therapeutic targets in IBD, signifying the discovery of novel and additional targets with therapeutic potential (figure 4A–B, online supplemental table 6). Fifty genes

were further identified as druggable based on annotation (from only one parent resource of druggability from the DGIdb (figure 4A–B, online supplemental table 6). By raising the druggability threshold to two sources, the number of potential druggable targets is reduced to eight (*TNFAIP3*, *PTGER4*, *GPR183*, *CXCR4*, *NR1D2*, *PRKCQ*, *SLC30A1* and *SOCS1*).

5.6% of the disease location signature genes were identified as druggable (online supplemental table 6). These include UC-downregulated genes encoding proteins such as *TNFAIP3* (absolute log₂FC UC vs L1=−1.06; FDR=0.001; figure 3C), *PTGER4*, *GPR183*, *NR1D2*, *SIRT1* and *PRKCQ*. Of these, *SIRT1* and *PTGER4* were identified to have potential adverse reactions when targeted (online supplemental table 6). However, genes (*BCL6*, *CDKN1A*, *BTG1*, *GADD45A*, *KLF4*) (figure 3A–C) within the down-regulated FOXO-pathway (which was one among the pathways consistently found to be over-represented among feature sets inferred by multiple methods) have not yet been targeted in IBD as well as other IMIDs (PS, RA, SC and SA). Although many of the disease location-associated genes with the strongest expression differences between UC and ileal CD patients were unsurprisingly involved in IBD pathogenesis, they present a potentially rewarding pool of therapeutic targets (figure 4C, online supplemental table 6). Examples include *TUBB2A* which is targeted in PS and RA and others such as *BCL6*, *NR4A2*, *DUSP10*, *NAPEPLD*, *PFKFB3*, *SRGN*, *SOCS3* and *SOCS1* which also exhibit differences between UC and non-IBD controls. Surprisingly, most of the (disease location signature) genes (20/24) with significant expression differences in the meta-analysis between UC patients and non-IBD controls displayed the opposite expression fold changes (downregulated in UC vs L1 and upregulated in UC vs non-IBD) (figure 4D).

As a complementary method, we also used the magnitude of the expression differences between ileal CD and UC patients to predict potential drugs for the specific subtypes of IBD defined by disease location. A reverse-effect screen (online supplemental table 7, online supplemental figure 10) resulted in the identification of possible drugs with a higher score (representative of the ability to modulate the expression signature) of 18.004 than a mimic-effect screen (0.294) (online supplemental figure 11, online supplemental table 8). Prominent modulators in the reverse-effect screen include agents such as withaferin-a, celastrol, narciclasine, ryuvidine, curcumin and mocetinostat among others (online supplemental table 7).

DISCUSSION

Disease location in patients with IBD carries a high degree of interpatient variability,⁴ although within a given patient it seems to be imprinted and genetically determined.⁵ Despite the underlying mechanisms which mediate location-specific phenotypic manifestations occur along the intestinal tract (the primary disease site), circulating immune cells and their expression signatures have been

used to predict disease and treatment outcomes.⁴⁸ In the current study, we performed transcriptomic profiling of monocytes and circulating CD4 T-cells purified from whole blood retrieved from CD and UC patients. Using a combination of supervised and unsupervised approaches, we investigated its link with disease location. Indeed, blood-derived CD4 T cell transcriptomics shed light on the two extremes of the IBD spectrum: UC and ileal CD with no significant differences observed between other sample groups with respect to disease location.

Instead of using a single methodology, we applied multiple methods (supervised and unsupervised) with different underlying theoretical bases to confirm whether results from different methods could converge into a common set of phenotypically relevant signals (figure 5). While differential expression analysis using DeSeq2 identified genes with a substantial variation in the mean expression between the ileal CD and UC patients, it does not consider codependencies such as coexpression of genes within a pathway or coexpression of genes between cell types. Hence, pathways enriched within the set of DEGs are expectedly sparse, and therefore provide little ground for comparison. In contrast, alternative methods (DIABLO) take into account not only the segregation of samples, but also their correlation with features from adjacent datasets (ie, the two gene expression datasets from the different cell types in our case). BioNERO, meanwhile, relies on the similarity of expression profiles among genes within the same dataset to infer modules of coexpressed genes. MOFA, by virtue of being an unsupervised method, identifies higher-order latent factors (equivalent to principal components in a PCA) representative of the expression profiles of the genes in each of the datasets. By associating the latent factors (via the weights assigned to the samples) to the clinical heterogeneity variables, we identified ‘explanatory’ latent factors. At the level of genes, about a quarter (24.55%) of the disease location-associated genes identified cumulatively were inferred by at least two different methods, thus bringing out the complementarity between the methods. As an additional validation step, we also compared the above-described signature to DEG-sets representing three distinct contexts at the tissue level (A) CD L1 inflamed ileum vs control ileum (B) UC inflamed colon vs control colon and (C) CD L1 inflamed ileum versus UC inflamed colon. Eventhough the validation datasets were not derived from the same cohort of patients, 44% of the DEGs (in CD4 T cells) distinguishing CD L1 and UC patients were also modulated in at least one validation dataset (online supplemental figure 12).

Additionally, at the level of pathways, we observed several ones which are over-represented within the disease location-associated gene sets identified by multiple methods. For example, pathway enrichment analysis within the circulating CD4 T cell transcriptome highlighted MAPK-associated pathways, FOXO-pathways in the differentiation between UC and ileal CD, which simultaneously popped-up through additional

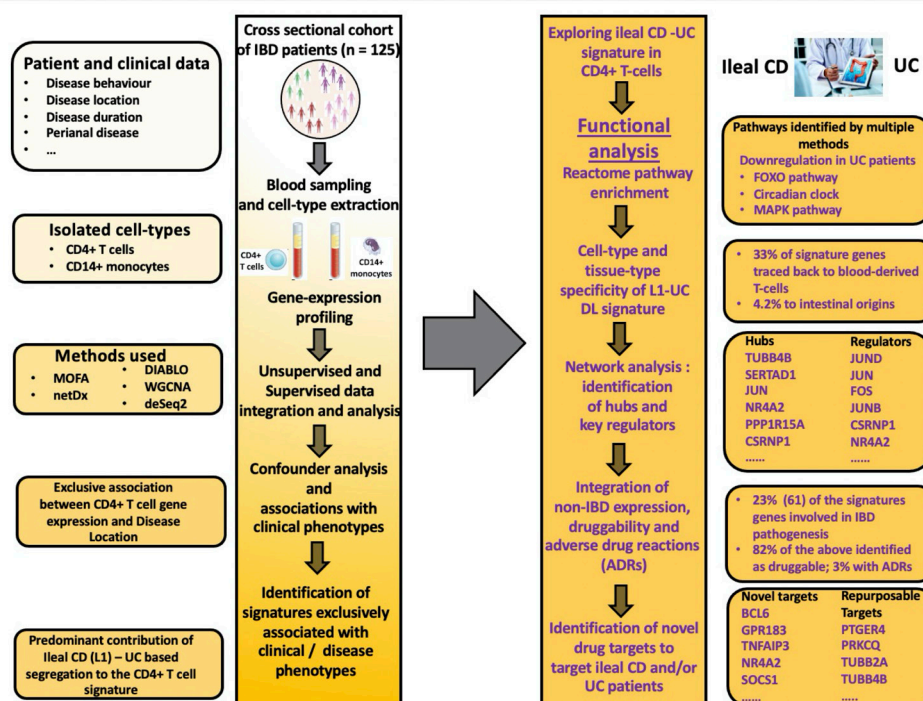


Figure 5 Summary of the workflow and results from the study. CD, Crohn's disease; IBD, inflammatory bowel disease; UC, ulcerative colitis.

unsupervised and supervised analytical approaches and was further confirmed by coexpression-based gene modules. Although no direct comparisons have previously been made between ileal CD and UC patients based on peripheral gene expression, the modulation of the MAPK pathways in UC is supported by earlier experimental studies.^{49–51} In contrast with all the aforementioned supervised methods, netDx uses the underlying pathway structures as meta-features to interpret and integrate the gene expression signals from the same dataset. In agreement with the over-representation of MAPK and FOXO pathways among the other supervised methods, netDx also captured the same pathways among the meta-level features (AUROC=86%) segregating ileal CD and UC patients.

Another discriminative pathway which was identified as a prominent feature by multiple methods is the FOXO transcriptional pathway, which based on our data seems key in ileal CD patients. The FOXO family of transcription factors such as FOXO3 are implicated in IBD pathology⁵² and the regulation of intestinal homeostatic processes such as inflammation, autophagy, mucus secretion, microbe–host interactions and maintenance of the intestinal barrier integrity.^{53–56} GWAS data from CD patients suggested that the minor allele (rs12212067) mapped to the FOXO3 locus, affects disease burden and outcome.⁵² Besides, members of the FOXO pathway, which we found to be downregulated in UC patients, are also expressed in lower levels in UC patients compared with non-IBD controls.⁵⁷ Although it cannot be confirmed independently using our own data alone (due to the lack of healthy/non-IBD samples in our study), the above observations suggest that the FOXO

pathway could be downregulated by a bigger margin in UC than ileal CD when compared with healthy controls, which is in line with the suggested stratification of IBD using genetic data.⁵ However, we did not find any evidence from publicly available resources for a basal intestinal expression of the FOXO pathway in the non-IBD/healthy context. The above combination of evidence suggests that the modulation of the FOXO pathway could be part of a molecular phenotype associated with the pathogenesis at the primary disease site(s), although further independent validation in larger cohorts is warranted. Although it is not clear if and how the ileal phenotype affects the potential relationship between IBD disease burden and the FOXO3 mutation, the refractory nature of ileal CD⁵⁸ as manifested across multiple clinical trials and additional meta-analysis^{59, 60} suggests that novel targets are indeed required. FOXO pathway members (*BCL6*, *CDKN1A*, *BTG1*, *GADD45A*, *KLF4*) which are upregulated in ileal CD patients, could potentially fill this therapeutic gap (table 2). None of them have yet been targeted in clinical trials for IBD or the other IMIDs. *BCL6* builds a compelling case as a potential novel target for ileal CD, since it modulates follicular helper T-cells, follicular regulatory T-cells⁶¹ in IBD, controls the inflammatory activity of regulatory T-cells,⁶² and drives the formation of the Th17 lineage of T-cells⁶³ which characterise ileal CD.⁶⁴ However, despite its potential disease relevance, further investigations need to be carried out to ascertain the (side)effects on other T-cell lineages when *BCL6* would be targeted.

We also identified several already used targets which could be potentially repurposed to treat ileal CD. These include *TUBB2A*, *TUBB4B* and *PRKCQ* which are targeted in PS and *PTGER4* which is targeted in RA. *TUBB2A*,

Table 2 Proposed targets for therapeutic targeting in UC and/or ileal CD.

Protein name	General functions	Transcription factor	UC versus L1 expression trend	UC versus non-IBD expression trend	Druggability (two sources)	Module hub?	Drugs targeting the protein (Disease–Clinical Trial ID)	ADRs
TUBB2A (Tubulin beta-2A chain)	Key mediator in the pathogenesis of PSC-IBD ⁶⁵	No	DOWN	–	No	No	Paclitaxel (Psoriasis–NCT00006276)	No
TUBB4B (Tubulin beta-4B chain)	Tubulin reorganisation ⁸⁵	No	DOWN	–	No	Yes	Paclitaxel (Psoriasis–NCT00006276)	No
TNFAIP3 (Tumour necrosis factor alpha-induced protein 3)	Master switch mediating anti-inflammatory feedback loop in CD4+ T cells ⁸⁶ ; Modulates intestinal autophagic response and inflammatory signalling ⁸⁷	No	DOWN	–	Yes	No	–	No
GPR183 (G-protein coupled receptor 183)	Upregulated in CD4 T cells during inflammation ⁸⁸ ; Regulation of interferon and autophagy activity ⁸⁹ ; Promotes interaction of CD4 T cells with other immune cell-types ⁹⁰	No	DOWN	UP	Yes	No	–	No
PRKQC (Protein kinase C theta type)	IBD susceptibility loci ³⁸ ; Modulation of T-cell differentiation and regulation of T-cell functions ⁹¹	No	DOWN	–	Yes	No	Sotrastaurin (Ulcerative colitis –NCT00572585); Sotrastaurin (Psoriasis–CT00885196)	No
SOC31 (Suppressor of cytokine signalling 1)	Modulates IFN-gamma and IL-4 dependent IBD pathogenesis ⁹³ ; Downregulation in T cells of patients with IBD ⁹⁴ ; Mediation of type-1 IFN-STAT1 signalling ⁹⁴ ; Regulator of intestinal immune tolerance ⁹⁵	No	DOWN	UP	Yes	No	–	No
PTGER4 (Prostaglandin E2 receptor EP4 subtype)	Significant association between PTGER4 variants and CD ³⁹ ; promotion of IFN-gamma producing Th1 and IL-17 producing Th17 cells ⁹⁶	No	DOWN	–	No	No	Rivenprost (Ulcerative colitis–NCT00296556); CR-6086 (Rheumatoid arthritis–NCT03163966)	Yes
SLC2A3 (Solute carrier family 2, facilitated glucose transporter member 3)	Expressed in resting ⁹⁷ and activated CD4 T cells ⁹⁸	No	DOWN	UP	No	Yes	–	No
NR4A2 (Nuclear receptor subfamily 4 group member 2 protein)	Regulates differentiation of CD4 T cells ⁹⁹ ; intermediated marker for macrophage activation ¹⁰⁰ ; modulation of MIF and MAPK signalling ¹⁰¹ ; T-cell homeostatic functions ⁹⁷	Yes	DOWN	UP	No	Yes	–	No
CXCR4 (C-X-C chemokine receptor type 4)	Participates in epithelial barrier responses ¹⁰² ; Expressed in T cells on exposure to Th2 cytokines ¹⁰³ ; Downregulated in T cells during leucocyte removal filter (LCAP) therapy in UC patients ¹⁰⁴	No	DOWN	UP	Yes	No	–	No
BCL6 (B-cell lymphoma 6 protein)	T-cell proliferation in patients with IBD ⁶¹ ; Mediates ATF3-dependent protection against colitis ¹⁰⁵	Yes	DOWN	UP	No	No	–	No
ADR, adverse drug reaction; CD, Crohn's disease; IBD, inflammatory bowel disease; LCAP, Leukocytapheresis; PSC, primary sclerosing cholangitis; UC, ulcerative colitis.								

upregulated in ileal CD in our study, was also identified as a key potential mediator in the pathogenesis of PSC.⁶⁵ Although PRKCQ and PTGER4 have been used as targets in UC, they have not yet been tested in (ileal) CD.

Beyond pathway representations, we identified regulators and regulatory mechanisms influencing pathway activities in the circulating CD4 T-cells differentiating ileal CD from UC patients. The inferred regulatory network led to the identification of key regulators such as *JUND*, *JUN*, *FOS*, *JUNB*, *KLF6*, *NR4A1*, *NR4A2*, *EGR1*, *KLF2* and *KLF9*. Most of these regulators, with the exception of *EGR1* and *NR4A1*, do not display any large difference in terms of transcriptional activity (as determined by the conservative criteria of differential expression) between the two patient groups, suggesting that they could be post-translationally modified and thereby change gene expression. Besides their documented roles in maintaining T cell functions,^{66 67} some of them like *EGR1*, *JUN* and *FOS* were also found to act in concert with the MAPK signalling pathway,^{68 69} suggesting the exertion of a concerted effect on the clinical phenotype. However, none of the TFs driving the expression of the disease location-associated genes are targeted either in IBD or the four IMIDs considered. This could be due to the intrinsic difficulty of targeting transcription factors in general which are usually localised within the nucleus. Nevertheless, the advent of novel molecules like anti-sense oligonucleotides⁷⁰ opens up the possibility of expanding the applicability of transcription factors as drug targets for IBD. Moreover, *NR4A1* and *NR4A2* (which is both a hub gene involved in IBD pathogenesis as well as being upregulated in ileal CD vs UC) belong to the category of nuclear receptors which are a class of transcription factors known for their potential therapeutic efficacies in IBD.⁷¹

Despite the significance of our findings, we acknowledge several pitfalls to our study. First, we have not profiled the wide-variety of cell types which could be involved in the pathogenesis of IBD in general and rather focused on two cell types, one from each arm of the immune system. Second, we profiled gene expression from purified cell-types derived from the peripheral blood of patients with IBD. Since the primary disease site(s) were excluded for sampling, the source of the signals could not be attributed to the primary sites. Third, we did not consider other omic layers which are known to be associated with disease location-associated phenotypes. Furthermore, more granular phenotypes such as disease extent (E1, E2, E3), especially for UC patients was not incorporated into the analysis. Finally, independent validation in larger cohorts with balanced sample numbers for each of the disease subtypes (ileal CD, ileocolonic CD, colonic CD and UC) and comparison with healthy controls at the level of the investigated cell types need to be performed.

CONCLUSION

In the current study, we harnessed a bioinformatic approach combining supervised and unsupervised analyses underpinning both extremes of the disease location spectrum through circulating monocytes and CD4 T

cell transcriptomics. We observed that disease location in patients with IBD tend to have a more pronounced imprintation on the expression of circulating CD4 T-cells than monocytes. We report specific mechanisms including key regulators and hubs in blood derived CD4 T cell which could potentially drive the expression differences observed between ileal CD and UC patients. Our study provides an initial glimpse into the molecular differences of both entities and paves the way for novel drug targets.

Acknowledgements The authors would like to acknowledge the funding agencies (FWO, ERC) for the financial support during this project.

Contributors BV and PS performed the data processing and writing of the manuscript. SV and JC contributed to generating the datasets used. JS, MF, and SV contributed to the critical revision of the manuscript and provided clinical inputs. PS is the guarantor of this manuscript.

Funding B Verstockett is supported by a Clinical Research Fund (KOOR) from the University Hospitals Leuven and the Research Council KU Leuven, Belgium. S Verstockett is a postdoctoral researcher and J Sabino and M Ferrante are Senior Clinical Investigators of Fonds Wetenschappelijk Onderzoek (FWO), Flanders, Belgium. S Vermeire is supported by a BOF-ZAP from KU Leuven, Belgium. PS is supported by the ERC Advanced Grant ERC-2015-AdG 694679.

Competing interests B Verstockett reports research support for research from Pfizer, speaker's fees from Abbvie, Biogen, Bristol Myers Squibb, Chiesi, Falk, Ferring, Galapagos, Janssen, MSD, Pfizer, R-Biopharm, Takeda, Truvion and Viartis and consultancy fees from Abbvie, Alimientiv, Applied Strategic, Atheneum, Bristol Myers Squibb, Galapagos, Guidepoint, Ipsos, Janssen, Progenity, Sandoz, Sosei Heptares, Takeda, Tillots Pharma and Viartis. SV has received research support from AbbVie, Johnson & Johnson, Pfizer, and Takeda; lecture fees from AbbVie, Centocor, Ferring, Genentech/Roche, Hospira, Johnson & Johnson, Merck Sharp & Dohme, Pfizer, Takeda, and Tillotts; and consulting fees from AbbVie, Abivax, Celgene, Celltrion, Centocor, Ferring, Galapagos, Genentech/Roche, Gilead, GlaxoSmithKline, Hospira, Johnson & Johnson, Merck Sharp & Dohme, Mundipharma, Pfizer, ProDigest, Prometheus, Second Genome, Takeda, and Tillotts. JS reports lecture fees from Abbvie, Takeda, Janssen, and Nestle Health Sciences. MF reports financial support for: research from AbbVie, Amgen, Biogen, Janssen, Pfizer, Takeda; consultancy from Abbvie, Boehringer-Ingelheim, Lilly, MSD, Pfizer, Sandoz, Takeda, and Thermo Fisher; speaking from Abbvie, Amgen, Biogen, Boehringer-Ingelheim, Falk, Ferring, Janssen, Lampro, MSD, Mylan, Pfizer, Sandoz, Takeda, and Truvion Healthcare. JC, SaV and PS do not have any conflicts to disclose.

Patient consent for publication Not applicable.

Ethics approval This study involves human participants and was approved by All included patients had given written consent to participate in the Institutional Review Board approved IBD Biobank (B322201213950/S53684 – Leuven) Participants gave informed consent to participate in the study before taking part.

Provenance and peer review Not commissioned; externally peer reviewed.

Data availability statement All data relevant to the study are included in the article or uploaded as supplementary information.

Supplemental material This content has been supplied by the author(s). It has not been vetted by BMJ Publishing Group Limited (BMJ) and may not have been peer-reviewed. Any opinions or recommendations discussed are solely those of the author(s) and are not endorsed by BMJ. BMJ disclaims all liability and responsibility arising from any reliance placed on the content. Where the content includes any translated material, BMJ does not warrant the accuracy and reliability of the translations (including but not limited to local regulations, clinical guidelines, terminology, drug names and drug dosages), and is not responsible for any error and/or omissions arising from translation and adaptation or otherwise.

Open access This is an open access article distributed in accordance with the Creative Commons Attribution 4.0 Unported (CC BY 4.0) license, which permits others to copy, redistribute, remix, transform and build upon this work for any purpose, provided the original work is properly cited, a link to the licence is given, and indication of whether changes were made. See: <https://creativecommons.org/licenses/by/4.0/>.

ORCID iDs

Bram Verstockt <http://orcid.org/0000-0003-3898-7093>

Sare Verstockt <http://orcid.org/0000-0001-6222-8527>

Padhmanand Sudhakar <http://orcid.org/0000-0003-1907-4491>

REFERENCES

- GBD 2017 Inflammatory Bowel Disease Collaborators. The global, regional, and national burden of inflammatory bowel disease in 195 countries and territories, 1990–2017: a systematic analysis for the global burden of disease study 2017. *Lancet Gastroenterol Hepatol* 2020;5:17–30.
- Ananthakrishnan AN, Bernstein CN, Iliopoulos D, et al. Environmental triggers in IBD: a review of progress and evidence. *Nat Rev Gastroenterol Hepatol* 2018;15:39–49.
- Atreya R, Siegmund B. Location is important: differentiation between ileal and colonic Crohn's disease. *Nat Rev Gastroenterol Hepatol* 2021;18:544–58.
- Verstockt B, Bressler B, Martinez-Lozano H. Time to revisit disease classification in IBD: is the current classification of IBD good enough for optimal clinical management? *Gastroenterology* 2022;162:1370–82. doi:10.1053/j.gastro.2021.12.246
- Cleynen I, Boucher G, Jostins L, et al. Inherited determinants of Crohn's disease and ulcerative colitis phenotypes: a genetic association study. *Lancet* 2016;387:156–67.
- Kredel LI, Jödicke LJ, Scheffold A, et al. T-cell composition in ileal and colonic creeping fat - Separating ileal from colonic Crohn's disease. *J Crohns Colitis* 2019;13:79–91.
- Biasci D, Lee JC, Noor NM, et al. A blood-based prognostic biomarker in IBD. *Gut* 2019;68:1386–95.
- Verstockt S, Verstockt B, Vermeire S. Oncostatin M as a new diagnostic, prognostic and therapeutic target in inflammatory bowel disease (IBD). *Expert Opin Ther Targets* 2019;23:943–54.
- Palmer NP, Silvester JA, Lee JJ, et al. Concordance between gene expression in peripheral whole blood and colonic tissue in children with inflammatory bowel disease. *PLoS One* 2019;14:e0222952.
- Maeda K, Nakamura M, Yamamura T, et al. Gelsolin as a potential biomarker for endoscopic activity and mucosal healing in ulcerative colitis. *Biomedicine* 2022;10. doi:10.3390/biomedicine10040872. [Epub ahead of print: 09 04 2022].
- Planell N, Masamunt MC, Leal RF, et al. Usefulness of transcriptional blood biomarkers as a non-invasive surrogate marker of mucosal healing and endoscopic response in ulcerative colitis. *J Crohns Colitis* 2017;11:1335–46.
- Gaujoux R, Starosvetsky E, Maimon N, et al. Cell-centred meta-analysis reveals baseline predictors of anti-TNF α non-response in biopsy and blood of patients with IBD. *Gut* 2019;68:604–14.
- Hegazy AN, West NR, Stubbington MJT, et al. Circulating and tissue-resident CD4⁺ T Cells with reactivity to intestinal microbiota are abundant in healthy individuals and function is altered during inflammation. *Gastroenterology* 2017;153:e16:1320–37.
- Zamora C, Canto E, Nieto JC, et al. Inverse association between circulating monocyte-platelet complexes and inflammation in ulcerative colitis patients. *Inflamm Bowel Dis* 2018;24:818–28.
- Ortega Moreno L, Fernández-Tomé S, Chaparro M, et al. Profiling of human circulating dendritic cells and monocyte subsets discriminates between type and mucosal status in patients with inflammatory bowel disease. *Inflamm Bowel Dis* 2021;27:268–74. doi:10.1093/ibd/izaa151
- Sudhakar P, Verstockt B, Cremer J, et al. Understanding the molecular drivers of disease heterogeneity in Crohn's disease using multi-omic data integration and network analysis. *Inflamm Bowel Dis* 2021;27:870–86. doi:10.1093/ibd/izaa281
- Kim D, Langmead B, Salzberg SL. HISAT: a fast spliced aligner with low memory requirements. *Nat Methods* 2015;12:357–60.
- Anders S, Pyl PT, Huber W. HTSeq—a Python framework to work with high-throughput sequencing data. *Bioinformatics* 2015;31:166–9.
- Argelaguet R, Velten B, Arnol D, et al. Multi-Omics Factor Analysis—a framework for unsupervised integration of multi-omics data sets. *Mol Syst Biol* 2018;14:e8124.
- Almeida-Silva F, Venancio TM. BioNERO: an all-in-one R/Bioconductor package for comprehensive and easy biological network reconstruction. *BioRxiv*. doi:10.1101/2021.04.10.439287
- Love MI, Huber W, Anders S. Moderated estimation of fold change and dispersion for RNA-seq data with DESeq2. *Genome Biol* 2014;15:550.
- Rohart F, Gautier B, Singh A, et al. mixOmics: An R package for 'omics feature selection and multiple data integration. *PLoS Comput Biol* 2017;13:e1005752.
- Pai S, Hui S, Isserlin R, et al. netDx: interpretable patient classification using integrated patient similarity networks. *Mol Syst Biol* 2019;15:e8497.
- Yu G, He Q-Y. ReactomePA: an R/Bioconductor package for reactome pathway analysis and visualization. *Mol Biosyst* 2016;12:477–9.
- Yu G, Wang L-G, Han Y, et al. clusterProfiler: an R package for comparing biological themes among gene clusters. *OMICS* 2012;16:284–7.
- Langfelder P, Horvath S. WGCNA: an R package for weighted correlation network analysis. *BMC Bioinformatics* 2008;9:559.
- Keenan AB, Torre D, Lachmann A, et al. ChEAS: transcription factor enrichment analysis by orthogonal omics integration. *Nucleic Acids Res* 2019;47:W212–24.
- Diehl AG, Boyle AP. Deciphering encode. *Trends Genet* 2016;32:238–49.
- Chèneby J, Ménétrier Z, Mestdagh M, et al. ReMap 2020: a database of regulatory regions from an integrative analysis of human and Arabidopsis DNA-binding sequencing experiments. *Nucleic Acids Res* 2020;48:D180–8.
- GTEx Consortium. The Genotype-Tissue expression (GTEx) project. *Nat Genet* 2013;45:580–5.
- Lachmann A, Torre D, Keenan AB, et al. Massive mining of publicly available RNA-seq data from human and mouse. *Nat Commun* 2018;9:1366.
- Thul PJ, Lindskog C. The human protein atlas: a spatial map of the human proteome. *Protein Sci* 2018;27:233–44.
- Linggi B, Jairath V, Zou G, et al. Meta-analysis of gene expression disease signatures in colonic biopsy tissue from patients with ulcerative colitis. *Sci Rep* 2021;11:18243.
- Carvalho-Silva D, Pierleoni A, Pignatelli M, et al. Open targets platform: new developments and updates two years on. *Nucleic Acids Res* 2019;47:D1056–65.
- Vancamelbeke M, Vanuytsel T, Farré R, et al. Genetic and transcriptomic bases of intestinal epithelial barrier dysfunction in inflammatory bowel disease. *Inflamm Bowel Dis* 2017;23:1718–29.
- Arijs I, De Hertogh G, Lemaire K, et al. Mucosal gene expression of antimicrobial peptides in inflammatory bowel disease before and after first infliximab treatment. *PLoS One* 2009;4:e7984.
- Arijs I, De Hertogh G, Machiels K, et al. Mucosal gene expression of cell adhesion molecules, chemokines, and chemokine receptors in patients with inflammatory bowel disease before and after infliximab treatment. *Am J Gastroenterol* 2011;106:748–61.
- Jostins L, Ripke S, Weersma RK, et al. Host-microbe interactions have shaped the genetic architecture of inflammatory bowel disease. *Nature* 2012;491:119–24.
- Di Narzo AF, Peters LA, Argmann C, et al. Blood and intestine eQTLs from an anti-TNF-resistant Crohn's disease cohort inform IBD genetic association loci. *Clin Transl Gastroenterol* 2016;7:e177.
- Freshour SL, Kiwala S, Cotto KC, et al. Integration of the drug-gene interaction database (DGIdb 4.0) with open crowdsourcing efforts. *Nucleic Acids Res* 2021;49:D1144–51.
- Tang J, Tanoli Z-U-R, Ravikumar B, et al. Drug target commons: a community effort to build a consensus knowledge base for drug-target interactions. *Cell Chem Biol* 2018;25:224–9.
- Szklarczyk D, Santos A, von Mering C, et al. Stitch 5: augmenting protein-chemical interaction networks with tissue and affinity data. *Nucleic Acids Res* 2016;44:D380–4.
- FDA Adverse Event Reporting System. FDA adverse event reporting system. Available: <https://open.fda.gov/data/faers/> [Accessed 31 Mar 2022].
- MedEffect. Available: <https://www.canada.ca/en/health-canada/services/drugs-health-products/medeffect-canada/medeffect-canada.html#a1> [Accessed 31 Mar 2022].
- Kuhn M, Letunic I, Jensen LJ, et al. The SIDER database of drugs and side effects. *Nucleic Acids Res* 2016;44:D1075–9.
- Offsides. Available: <http://tatonettillab.org/offsides/> [Accessed 31 Mar 2022].
- Duan Q, Reid SP, Clark NR, et al. L1000CDS2: LINCS L1000 characteristic direction signatures search engine. *NPJ Syst Biol Appl* 2016;2. doi:10.1038/npsba.2016.15. [Epub ahead of print: 04 08 2016].
- Verstockt B, Verstockt S, Dehairs J, et al. Low TREM1 expression in whole blood predicts anti-TNF response in inflammatory bowel disease. *EBioMedicine* 2019;40:733–42.
- Bai X-S, Bai G, Tang L-D, et al. MiR-195 alleviates ulcerative colitis in rats via MAPK signaling pathway. *Eur Rev Med Pharmacol Sci* 2020;24:2640–6.

- 50 Li YY, Yuece B, Cao HM, *et al.* Inhibition of p38/Mk2 signaling pathway improves the anti-inflammatory effect of WIN55 on mouse experimental colitis. *Lab Invest* 2013;93:322–33.
- 51 Setia S, Nehru B, Sanyal SN. Upregulation of MAPK/Erk and PI3K/Akt pathways in ulcerative colitis-associated colon cancer. *Biomed Pharmacother* 2014;68:1023–9.
- 52 Lee JC, Espélli M, Anderson CA, *et al.* Human SNP links differential outcomes in inflammatory and infectious disease to a FOXO3-regulated pathway. *Cell* 2013;155:57–69.
- 53 Yin Y, Wang J, Zhao X, *et al.* Overexpressed FOXO3 improves inflammatory status in mice by affecting NLRP3-mediated cell coronation in necrotizing colitis mice. *Biomed Pharmacother* 2020;125:109867.
- 54 Snoeks L, Weber CR, Wasland K, *et al.* Tumor suppressor FOXO3 participates in the regulation of intestinal inflammation. *Lab Invest* 2009;89:1053–62.
- 55 Han C, Guo L, Sheng Y, *et al.* FoxO1 regulates TLR4/MyD88/MD2-NF- κ B inflammatory signalling in mucosal barrier injury of inflammatory bowel disease. *J Cell Mol Med* 2020;24:3712–23.
- 56 Snoeks L, Weber CR, Turner JR, *et al.* Tumor suppressor Foxo3a is involved in the regulation of lipopolysaccharide-induced interleukin-8 in intestinal HT-29 cells. *Infect Immun* 2008;76:4677–85.
- 57 Min M, Yang J, Yang Y-S, *et al.* Expression of transcription factor FOXO3a is decreased in patients with ulcerative colitis. *Chin Med J* 2015;128:2759–63.
- 58 Tanida S, Ozeki K, Mizoshita T, *et al.* Managing refractory Crohn's disease: challenges and solutions. *Clin Exp Gastroenterol* 2015;8:131–40.
- 59 Dulai PS, Singh S, Vande Casteele N, *et al.* Should we divide Crohn's disease into ileum-dominant and isolated colonic diseases? *Clin Gastroenterol Hepatol* 2019;17:2634–43.
- 60 Srinivasan A, De Cruz P, van Langenberg DR. Letter: choosing between ustekinumab and vedolizumab in anti-TNF refractory Crohn's disease-the devil is in the detail. *Aliment Pharmacol Ther* 2020;52:561–2.
- 61 Yang Y, Lv X, Zhan L, *et al.* Case report: IL-21 and BCL-6 regulate the proliferation and secretion of Tfh and TFR cells in the intestinal germinal center of patients with inflammatory bowel disease. *Front Pharmacol* 2020;11:587445.
- 62 Sawant DV, Sehra S, Nguyen ET, *et al.* Bcl6 controls the Th2 inflammatory activity of regulatory T cells by repressing GATA3 function. *J Immunol* 2012;189:4759–69.
- 63 Kotov JA, Kotov DI, Linehan JL, *et al.* BCL6 corepressor contributes to Th17 cell formation by inhibiting Th17 fate suppressors. *J Exp Med* 2019;216:1450–64.
- 64 Visekruna A, Hartmann S, Silke YR, *et al.* Intestinal development and homeostasis require activation and apoptosis of diet-reactive T cells. *J Clin Invest* 2019;129:1972–83.
- 65 Quraishi MN, Acharjee A, Beggs AD, *et al.* A pilot integrative analysis of colonic gene expression, gut microbiota, and immune infiltration in primary sclerosing Cholangitis-inflammatory bowel disease: association of disease with bile acid pathways. *J Crohns Colitis* 2020;14:935–47.
- 66 Koizumi S-I, Sasaki D, Hsieh T-H, *et al.* JunB regulates homeostasis and suppressive functions of effector regulatory T cells. *Nat Commun* 2018;9:5344.
- 67 Liu X, Wang Y, Lu H, *et al.* Genome-wide analysis identifies NR4A1 as a key mediator of T cell dysfunction. *Nature* 2019;567:525–9.
- 68 Ten Hoeve AL, Hakimi M-A, Barragan A. Sustained Egr-1 response via p38 MAP kinase signaling modulates early immune responses of dendritic cells parasitized by *Toxoplasma gondii*. *Front Cell Infect Microbiol* 2019;9:349.
- 69 Zhang Y, Xu M, Zhang X, *et al.* MAPK/c-Jun signaling pathway contributes to the upregulation of the anti-apoptotic proteins Bcl-2 and Bcl-xL induced by Epstein-Barr virus-encoded BARF1 in gastric carcinoma cells. *Oncol Lett* 2018;15:7537–44.
- 70 Quemener AM, Centomo ML, Sax SL, *et al.* Small drugs, huge impact: the extraordinary impact of antisense oligonucleotides in research and drug development. *Molecules* 2022;27. doi:10.3390/molecules27020536. [Epub ahead of print: 15 Jan 2022].
- 71 Laverny G, Penna G, Vetrano S, *et al.* Efficacy of a potent and safe vitamin D receptor agonist for the treatment of inflammatory bowel disease. *Immunol Lett* 2010;131:49–58.
- 72 Wu H, Li X-M, Wang J-R, *et al.* NUR77 exerts a protective effect against inflammatory bowel disease by negatively regulating the TRAF6/TLR-IL-1R signalling axis. *J Pathol* 2016;238:457–69.
- 73 Sundberg TB, Choi HG, Song J-H, *et al.* Small-molecule screening identifies inhibition of salt-inducible kinases as a therapeutic strategy to enhance immunoregulatory functions of dendritic cells. *Proc Natl Acad Sci U S A* 2014;111:12468–73.
- 74 Masago K, Fujita S. Novel NR4A1 arg293ser mutation in patients with familial Crohn's disease. *In Vivo* 2021;35:2135–40.
- 75 Pulakazhi Venu VK, Alston L, Iftinca M, *et al.* Nr4A1 modulates inflammation-associated intestinal fibrosis and dampens fibrogenic signaling in myofibroblasts. *Am J Physiol Gastrointest Liver Physiol* 2021;321:G280–97.
- 76 Rawat M, Nighot M, Al-Sadi R, *et al.* IL1B increases intestinal tight junction permeability by up-regulation of MIR200C-3p, which degrades occludin mRNA. *Gastroenterology* 2020;159:1375–89.
- 77 Li Y, Liu M, Zuo Z, *et al.* TLR9 regulates the NF- κ B-NLRP3-IL-1 β pathway negatively in *Salmonella*-Induced NKG2D-mediated intestinal inflammation. *J Immunol* 2017;199:761–73.
- 78 Ma C, Wu W, Lin R, *et al.* Critical role of cd6highcd4+ T cells in driving Th1/Th17 cell immune responses and mucosal inflammation in IBD. *J Crohns Colitis* 2019;13:510–24.
- 79 Li H, Fan C, Feng C, *et al.* Inhibition of phosphodiesterase-4 attenuates murine ulcerative colitis through interference with mucosal immunity. *Br J Pharmacol* 2019;176:2209–26.
- 80 Minar P, Lehn C, Tsai Y-T, *et al.* Elevated pretreatment plasma oncostatin M is associated with poor biochemical response to infliximab. *Crohns Colitis* 2019;1:otz026.
- 81 Verstockt S, Verstockt B, Machiels K, *et al.* Oncostatin M is a biomarker of diagnosis, worse disease prognosis, and therapeutic nonresponse in inflammatory bowel disease. *Inflamm Bowel Dis* 2021;27:1564–75.
- 82 Mateos B, Sáez-González E, Moret I, *et al.* Plasma oncostatin M, TNF- α , IL-7, and IL-13 network predicts Crohn's disease response to infliximab, as assessed by calprotectin log drop. *Dig Dis* 2021;39:1–9.
- 83 Beigel F, Friedrich M, Probst C, *et al.* Oncostatin M mediates STAT3-dependent intestinal epithelial restitution via increased cell proliferation, decreased apoptosis and upregulation of serpin family members. *PLoS One* 2014;9:e93498.
- 84 West NR, Hegazy AN, Owens BMJ, *et al.* Oncostatin M drives intestinal inflammation and predicts response to tumor necrosis factor-neutralizing therapy in patients with inflammatory bowel disease. *Nat Med* 2017;23:579–89.
- 85 Janke C. The tubulin code: molecular components, readout mechanisms, and functions. *J Cell Biol* 2014;206:461–72.
- 86 Urbano PCM, Aguirre-Gamboa R, Ashikov A, *et al.* TNF- α -induced protein 3 (TNFAIP3)/A20 acts as a master switch in TNF- α blockade-driven IL-17A expression. *J Allergy Clin Immunol* 2018;142:517–29.
- 87 Serramito-Gómez I, Boada-Romero E, Slowicka K, *et al.* The anti-inflammatory protein TNFAIP3/A20 binds the WD40 domain of ATG16L1 to control the autophagic response, NFKB/NF- κ B activation and intestinal homeostasis. *Autophagy* 2019;15:1657–9.
- 88 Tischner D, Grimm M, Kaur H, *et al.* Single-cell profiling reveals GPCR heterogeneity and functional patterning during neuroinflammation. *JCI Insight* 2017;2. doi:10.1172/jci.insight.95063. [Epub ahead of print: 03 Aug 2017].
- 89 Bartlett S, Gemiarto AT, Ngo MD, *et al.* GPR183 regulates interferons, autophagy, and bacterial growth during *Mycobacterium tuberculosis* infection and is associated with TB disease severity. *Front Immunol* 2020;11:601534.
- 90 Li J, Lu E, Yi T, *et al.* EB12 augments Tfh cell fate by promoting interaction with IL-2-quenching dendritic cells. *Nature* 2016;533:110–4.
- 91 Kong K-F, Yokosuka T, Canonigo-Balancio AJ, *et al.* A motif in the V3 domain of the kinase PKC- θ determines its localization in the immunological synapse and functions in T cells via association with CD28. *Nat Immunol* 2011;12:1105–12.
- 92 Wang X, Chuang H-C, Li J-P, *et al.* Regulation of PKC- θ function by phosphorylation in T cell receptor signaling. *Front Immunol* 2012;3:197.
- 93 Chinen T, Kobayashi T, Ogata H, *et al.* Suppressor of cytokine signaling-1 regulates inflammatory bowel disease in which both IFN γ and IL-4 are involved. *Gastroenterology* 2006;130:373–88.
- 94 Giles EM, Sanders TJ, McCarthy NE, *et al.* Regulation of human intestinal T-cell responses by type 1 interferon-STAT1 signaling is disrupted in inflammatory bowel disease. *Mucosal Immunol* 2017;10:184–93.
- 95 Chinen T, Komai K, Muto G, *et al.* Prostaglandin E2 and SOCS1 have a role in intestinal immune tolerance. *Nat Commun* 2011;2:190.
- 96 Lee J, Aoki T, Thumkeo D, *et al.* T cell-intrinsic prostaglandin E2-EP2/EP4 signaling is critical in pathogenic TH17 cell-driven inflammation. *J Allergy Clin Immunol* 2019;143:631–43.

- 97 Macintyre AN, Gerriets VA, Nichols AG, *et al.* The glucose transporter GLUT1 is selectively essential for CD4 T cell activation and effector function. *Cell Metab* 2014;20:61–72.
- 98 Maratou E, Dimitriadis G, Kollias A, *et al.* Glucose transporter expression on the plasma membrane of resting and activated white blood cells. *Eur J Clin Invest* 2007;37:282–90.
- 99 Sekiya T, Kashiwagi I, Inoue N, *et al.* The nuclear orphan receptor NR4A2 induces FOXP3 and regulates differentiation of CD4+ T cells. *Nat Commun* 2011;2:269.
- 100 Barish GD, Downes M, Alaynick WA, *et al.* A nuclear receptor atlas: macrophage activation. *Mol Endocrinol* 2005;19:2466–77.
- 101 Ralph JA, Ahmed AU, Santos LL, *et al.* Identification of NURR1 as a mediator of MIF signaling during chronic arthritis: effects on glucocorticoid-induced MKP1. *Am J Pathol* 2010;177:2366–78.
- 102 Zimmerman NP, Vongsa RA, Faherty SL, *et al.* Targeted intestinal epithelial deletion of the chemokine receptor CXCR4 reveals important roles for extracellular-regulated kinase-1/2 in restitution. *Lab Invest* 2011;91:1040–55.
- 103 Annunziato F, Cosmi L, Galli G, *et al.* Assessment of chemokine receptor expression by human Th1 and Th2 cells in vitro and in vivo. *J Leukoc Biol* 1999;65:691–9.
- 104 Nakase H, Mikami S, Chiba T. Alteration of CXCR4 expression and Th1/Th2 balance of peripheral CD4-positive T cells can be a biomarker for leukocytapheresis therapy for patients with refractory ulcerative colitis. *Inflamm Bowel Dis* 2009;15:963–4.
- 105 Cao Y, Yang Q, Deng H, *et al.* Transcriptional factor ATF3 protects against colitis by regulating follicular helper T cells in Peyer's patches. *Proc Natl Acad Sci U S A* 2019;116:6286–91.

Variable	N	CD, N = 87 ¹	UC, N = 38 ¹	p-value ²
Gender	125			0.8
F		48 (55%)	22 (58%)	
M		39 (45%)	16 (42%)	
Age	125	36 (28, 49)	42 (28, 57)	0.2
Disease.duration	125	12 (4, 23)	7 (2, 14)	0.025
CRP	123	6 (3, 18)	2 (1, 8)	0.001
Previous.antiTNF.use	125	60 (69%)	23 (61%)	0.4
PreviousVDZ.use	125	32 (37%)	2 (5.3%)	<0.001
Disease.behaviour	87			
B1		34 (39%)	0 (NA%)	
B2		33 (38%)	0 (NA%)	
B3		20 (23%)	0 (NA%)	
Perianal.symptoms	87	36 (41%)	0 (NA%)	
Steroid.use	125			0.006
No		62 (71%)	22 (58%)	
Systemic		14 (16%)	2 (5.3%)	
Topical		11 (13%)	14 (37%)	
Smoking.status	125			0.033
Active-smoker		20 (23%)	2 (5.3%)	
Former-smoker		23 (26%)	16 (42%)	
Non-smoker		44 (51%)	20 (53%)	

¹ n (%); Median (IQR)

² Pearson's Chi-squared test; Wilcoxon rank sum test; Fisher's exact test

Gene	LF	Dataset	References
EMP1	LF1	CD14 transcriptomics	-
CX3CR1	LF1	CD14 transcriptomics	29743615;25024136;17285595;24625
RGCC	LF1	CD14 transcriptomics	-
NAMPTL	LF1	CD14 transcriptomics	-
NAMPT	LF1	CD14 transcriptomics	28877980;28837586;31179321
THBD	LF1	CD14 transcriptomics	23388545
NAB2	LF1	CD14 transcriptomics	-
B3GNT5	LF1	CD14 transcriptomics	-
HBEGF	LF1	CD14 transcriptomics	15749028;15300588
FOSL1	LF1	CD14 transcriptomics	23128233
PHLDA1	LF1	CD14 transcriptomics	-
HIF1A	LF1	CD14 transcriptomics	31063937;29307990;30098863
GIMAP8	LF1	CD14 transcriptomics	-
PFKFB3	LF1	CD14 transcriptomics	30541017
SLC7A5	LF1	CD14 transcriptomics	-
GPR183	LF1	CD14 transcriptomics	33511653;30742043
GOS2	LF1	CD14 transcriptomics	20848504;26339133
NRIP3	LF1	CD14 transcriptomics	-
ATP2B1	LF1	CD14 transcriptomics	17262812
SDC4	LF1	CD14 transcriptomics	30053064

Functional role or involvement in pathogenesis of IBD

- Recruitment of immune cells to disease site; maturation of immune cells; production of inflammation
-
- Upregulated in IBD; acts as a link between NAD metabolism and intestinal inflammation; Upregulated in UC patients with neoplasia compared to controls and UC patients without neoplasia
-
- Involved in IL-8 mediated signaling and cellular proliferation in the gut IBD susceptibility locus
-
- Involved in hypoxia response pathways in IBD
-
- Blood transcriptional biomarker for IBD
-
- SNP induced upregulation of expression in PBMCs of IBD patients; involved in intestinal pathogenesis
- Predictive biomarker for infliximab response in colonic CD; genetic marker for infliximab response
-
- Downregulated in UC compared to CD
- Involved in epithelial cell integrity and regeneration in colitis model

inflammatory cytokines; increased expression in IBD patients

hyperplasia

pathogenesis, inflammation and development of colitis
response

Gene	LF	Dataset	References	Functional role or involvement in patho
CISH	LF1	CD4 transcrip	-	-
BCL3	LF1	CD4 transcrip	20601676; 28	IBD susceptibility locus; development of
ARID5A	LF1	CD4 transcrip	27022145	Regulates naive CD4+ T cell fate
PIM3	LF1	CD4 transcrip	22078270;30	Plays a role in CD4 T cell activation and
PER1	LF1	CD4 transcrip	28710114;30	Involved in intestinal inflammation; act
PAQR8	LF1	CD4 transcrip	http://twas-	Identified as a TWAS gene for CD and U
PDE4D	LF1	CD4 transcrip	30883697	Intracellular proinflammatory enzyme, l
DUSP8	LF1	CD4 transcrip	-	-
PELI1	LF1	CD4 transcrip	19734906	Facilitates TRIF-dependent Toll-like rec
SLC7A5	LF1	CD4 transcrip	25701737	Involved in bacterial clearance in humar
FOSL2	LF1	CD4 transcrip	30397350	Part of a regulatory network correspon
CD200R1	LF1	CD4 transcrip	26690123	Decreased fraction of CD4+ T cells expre
WHAMM	LF1	CD4 transcrip	-	-
TNFAIP3	LF1	CD4 transcrip	29788367;33	IBD susceptibility locus; involved in resp
ST6GAL1	LF1	CD4 transcrip	-	-
FURIN	LF1	CD4 transcrip	30266770	Triggers for the Production of TGF- β by
RBM38	LF1	CD4 transcrip	-	-
PFKFB3	LF1	CD4 transcrip	27387960;22	Mediates intestinal inflammation
HIF1A	LF1	CD4 transcrip	31063937;29	Involved in hypoxia response pathways i
TRIM69	LF1	CD4 transcrip	-	-

genesis of IBD

f colitis

inflammatory bowel disease; IBD predisposition

s as a clock gene whose disruption is associated with the early onset of IBD

IC

hydrolyzing and inactivating cAMP and subsequently intestinal inflammation

eptor signaling and proinflammatory cytokine production

n IECs

ding to a wound-healing program mediated by CD161+ regulatory T (Treg) cells

essing CD200R1 in IBD patients

onse to anti-TNF treatment; master switch of cytokines such as IL-17

T Cells in the intestine

in IBD

Gene	LF	Dataset	References	Functional role or involvement
NR4A3	LF2	CD14 transcriptomics	-	-
IL1B	LF2	CD14 transcriptomics	32569770;28	Enhances intestinal tight junctions
CD69	LF2	CD14 transcriptomics	30395204	Plays a role in immune response
PDE4B	LF2	CD14 transcriptomics	30883697	Inhibition of PDE4 by aprepitant
OSM	LF2	CD14 transcriptomics	28368383;24	Drives intestinal inflammation
SNAI1	LF2	CD14 transcriptomics	-	-
EREG	LF2	CD14 transcriptomics	29129684	Regulation of intestinal homeostasis
PTGS2	LF2	CD14 transcriptomics	16273614	Haplotype of prostaglandin synthase
NR4A2	LF2	CD14 transcriptomics	-	-
ATF3	LF2	CD14 transcriptomics	30455690;32	Mediates a cross-regulatory network
GOS2	LF2	CD14 transcriptomics	20848504;26	Predictive biomarker for intestinal disease
OLR1	LF2	CD14 transcriptomics	-	-
IL8	LF2	CD14 transcriptomics	8801200;114	Inflammatory marker in IBD
NR4A1	LF2	CD14 transcriptomics	34182489;26	Susceptibility loci in familial Crohn's disease
CD83	LF2	CD14 transcriptomics	19095953;25	Involved in the dendritic cell maturation
MAFF	LF2	CD14 transcriptomics	-	-
CDKN1A	LF2	CD14 transcriptomics	-	-
BHLHE40	LF2	CD14 transcriptomics	29773643	Molecular switch for dendritic cell maturation
PHLDA1	LF2	CD14 transcriptomics	34349991	The expression levels of PHLDA1 in IBD
SLC7A5	LF2	CD14 transcriptomics	-	-

ment in pathogenesis of IBD

unction permeability

sponses and mucosal inflammation in IBD

milast protected against UC, by interfering with mucosal immunity;

tion and predicts response to tumor necrosis factor-neutralizing therapy; mediates STAT3-de

omeostasis and intestinal stem cell regeneration

n synthase 2/cyclooxygenase 2 is involved in the susceptibility to inflammatory bowel disease

on in the barrier to maintain mucosal homeostasis and immunity; important regulator of folli

ifliximab response in colonic CD; genetic marker for infliximab response

IBD patients: IBD pathogenesis; susceptibility gene in inflammatory bowel disease patients; pri

ial CD; protective effect against inflammatory bowel disease; modulates inflammation-associa

ell pathogenesis in CD patients; Dendritic cell CD83 homotypic interactions regulate inflammat

rmining the fate of inflammatory and antiinflammatory Th1 cells.

HLDA1 in UC cases were higher in colitis, followed by dysplasia and UC-CRC, which suggested

pendent intestinal epithelial restitution; Predicts Crohn's Disease Response to Infliximab; bio

!

cular helper T (TFH) cells in gut; protects against colitis by regulating follicular helper T (TFH)

redictors of response to Vedolizumab in Inflammatory Bowel Diseases

ited intestinal fibrosis and dampens fibrogenic signaling in myofibroblasts

tion and promote mucosal homeostasis; reduced number of CD83 positive dendritic cells in CI

that this protein may be involved in the carcinogenesis of UC-CRC

narker for diagnosis; Poor Biochemical Response to Infliximab

cells in the gut;promotes intestinal epithelial cell apoptosis in Crohn's disease

3 patients;Difference in Presence and Number of CD83 + Dendritic Cells in Patients with Ulcer

ative Colitis and Crohn's Disease

Gene	LF	Dataset	References	Functional role or involvement in patho
NR4A2	LF2	CD4 transcrip	26564988	Protective effect against inflammatory
CSRN1	LF2	CD4 transcrip -	-	-
SIK1	LF2	CD4 transcrip	25114223	Identified as a possible drug target for c
FOSB	LF2	CD4 transcrip -	-	-
NR4A1	LF2	CD4 transcrip	34182489;34	Susceptibility loci in a Japanese family \
CDKN1A	LF2	CD4 transcrip -	-	-
PPP1R15A	LF2	CD4 transcrip -	-	-
SLC2A3	LF2	CD4 transcrip	31618209	One among six genes whose expression
JUN	LF2	CD4 transcrip	12223450	Involved in the pathogenic mechanisms
MYADM	LF2	CD4 transcrip -	-	-
MIDN	LF2	CD4 transcrip -	-	-
ZFP36	LF2	CD4 transcrip	34380509	Involved in intestinal mucosal homeost
SMAD7	LF2	CD4 transcrip	31553906;11	Controls Immunoregulatory PDL2/1-PD1
TNFAIP3	LF2	CD4 transcrip	29788367;33	IBD susceptibility locus; involved in resp
TOB2	LF2	CD4 transcrip	33247598	Over-expressed in the colonic mucosa o
FOS	LF2	CD4 transcrip -	-	-
RGS1	LF2	CD4 transcrip	21795595	Involved in gut T cell trafficking
FAM46C	LF2	CD4 transcrip -	-	-
PTGER4	LF2	CD4 transcrip	33558271	Prostaglandin E 2 receptor PTGER4-expi
YPEL5	LF2	CD4 transcrip	33963246	Correlation between methylation abnor

genesis of IBD

bowel disease by negatively regulating the TRAF6/TLR-IL-1R signalling axis

colitis based on small-molecule screening

with CD; modulates inflammation-associated intestinal fibrosis and dampens fibrogenic signa

l levels in blood differentiated IBD patients from non-IBD controls
associated with steroid unresponsiveness in CD patients

asis

l Signaling in Intestinal Inflammation and Autoimmunity;Blocking Smad7 restores TGF-beta1
onse to anti-TNF treatment; master switch of cytokines such as IL-17
f patients with UC in remission compared with the active UC and control group

ressing macrophages promote intestinal epithelial barrier regeneration upon inflammation
malities and expression patterns in CD patients

aling in myofibroblasts

signaling in chronic inflammatory bowel disease

Gene	Set	IBD_lit_search	Barrier gene: AMP genes	Cell adhesior
PPP1R15A	DIABLO-LF2-mods	NA	NA	NA
AMD1	LF2_mods	NA	NA	NA
ATF3	DEGs-DIABLO-LF2-Mods	NA	NA	NA
ATF4	LF2_mods	NA	NA	NA
AVPI1	DIABLO-LF2	NA	NA	NA
B3GNT2	DIABLO-LF2		1	NA
BBX	LF2_mods		1	NA
BCL6	DEGs-DIABLO-LF2		1	NA
BCOR	LF2_mods	NA	NA	NA
BRD2	LF2_mods	NA	NA	NA
BTG1	DIABLO-LF2-mods	NA	NA	NA
BTG2	DIABLO-LF2-mods		1	NA
CD69	LF2_mods		1	NA
CD83	DEGs-DIABLO-LF2		1	NA
CDKN1A	DEGs-DIABLO-LF2-Mods		1	NA
CHMP1B	DIABLO-LF2-mods	NA	NA	NA
CITED2	LF2_mods	NA	NA	NA
CKS2	LF2_mods	NA	NA	NA
CLK1	LF2_mods	NA	NA	NA
CREM	DEGs-DIABLO-LF2		1	NA
CXCR4	LF2_mods		1	NA
CYCS	DIABLO-LF2-mods		1	NA
DDIT3	LF2_mods		1	NA
DNAJA1	DIABLO-LF2-mods	NA	NA	NA
DUSP1	LF2_mods	NA	NA	NA
DUSP10	DEGs-DIABLO-LF2-Mods	NA	NA	NA
DUSP2	DIABLO-LF2-mods		1	NA
DUSP4	DIABLO-LF2		1	NA
DUSP5	DIABLO-LF2	NA	NA	NA
DUSP6	DIABLO-LF2		1	NA
DYNLL1	LF2_mods	NA	NA	NA
EGR2	DEGs-DIABLO-LF2-Mods		1	NA
EGR3	DEGs-LF2-mods	NA	NA	NA
EIF4A3	LF2_mods	NA	NA	NA
EIF5	LF2_mods		1	NA
ERRFI1	LF2_mods	NA	NA	NA
FOS	LF2_mods		1	NA
FOSB	LF2_mods		1	NA
FOSL2	DEGs-DIABLO-LF2		1	NA
FOXJ1	LF2_mods		1	NA
FZD7	LF2_mods		1	NA
G3BP2	DIABLO-LF2		1	NA
GADD45A	DIABLO-LF2-mods	NA	NA	NA
GADD45B	LF2_mods	NA	NA	NA
GADD45G	LF2_mods	NA	NA	NA
GLA	LF2_mods		1	NA
GPR183	DIABLO-LF2		1	NA

GTF2B	DIABLO-LF2	NA		NA	NA	NA
HBEGF	DEGs-LF2		1	NA	NA	NA
HSP90AA1	LF2_mods	NA		NA	NA	NA
HSPA1B	LF2_mods	NA		NA	NA	NA
HSPA2	LF2_mods		1	NA	NA	NA
HSPA5	DIABLO-LF2		1	NA	NA	NA
HSPA8	LF2_mods	NA		NA	NA	NA
HSPH1	LF2_mods	NA		NA	NA	NA
ID1	DIABLO-LF2-mods	NA		NA	NA	NA
ID2	LF2_mods	NA		NA	NA	NA
ID3	LF2_mods	NA		NA	NA	NA
IDI1	LF2_mods	NA		NA	NA	NA
IER2	LF2_mods	NA		NA	NA	NA
IER5	LF2_mods	NA		NA	NA	NA
IFRD1	LF2_mods		1	NA	NA	NA
IRF1	DIABLO-LF2	NA		NA	NA	NA
IRF2BPL	LF2_mods	NA		NA	NA	NA
IRS2	DIABLO-LF2-mods	NA		NA	NA	NA
JOSD1	DIABLO-LF2	NA		NA	NA	NA
JUN	LF2_mods		1	NA	NA	NA
JUNB	LF2_mods	NA		NA	NA	NA
JUND	LF2_mods	NA		NA	NA	NA
KAT7	DIABLO-LF2	NA		NA	NA	NA
KBTBD8	LF2_mods	NA		NA	NA	NA
KLF10	DIABLO-LF2		1	NA	NA	NA
KLF11	DIABLO-LF2	NA		NA	NA	NA
KLF16	LF2_mods	NA		NA	NA	NA
KLF2	LF2_mods		1	NA	NA	NA
KLF4	DEGs-DIABLO-LF2		1	NA	NA	NA
KLF5	LF2_mods		1	NA	NA	NA
KLF6	LF2_mods		1	NA	NA	NA
KLF9	LF2_mods	NA		NA	NA	NA
KLHL15	DIABLO-LF2-mods	NA		NA	NA	NA
KPNA2	DIABLO-LF2-mods	NA		NA	NA	NA
LBH	LF2_mods	NA		NA	NA	NA
LDHA	DIABLO-LF2	NA		NA	NA	NA
LIMD1	DIABLO-LF2		1	NA	NA	NA
LMNA	DEGs-LF2-mods	NA		NA	NA	NA
MAFF	DIABLO-LF2	NA		NA	NA	NA
MARCKSL1	LF2_mods	NA		NA	NA	NA
MAT2A	LF2_mods	NA		NA	NA	NA
MDM4	LF2_mods	NA		NA	NA	NA
MEPCE	LF2_mods	NA		NA	NA	NA
MT-ATP6	LF2_mods	NA		NA	NA	NA
MT-CO1	LF2_mods	NA		NA	NA	NA
MT-CO2	LF2_mods	NA		NA	NA	NA
MT-CO3	LF2_mods	NA		NA	NA	NA
MT-ND1	LF2_mods	NA		NA	NA	NA

MT-ND2	LF2_mods	NA		NA	NA	NA
MT-ND3	LF2_mods	NA		NA	NA	NA
MT-ND4	LF2_mods	NA		NA	NA	NA
MT-ND4L	LF2_mods	NA		NA	NA	NA
MT-ND5	LF2_mods	NA		NA	NA	NA
MTRNR2L8	LF2_mods	NA		NA	NA	NA
MXD1	LF2_mods	NA		NA	NA	NA
MYLIP	LF2_mods		1	NA	NA	NA
NAMPT	DIABLO-LF2	NA		NA	NA	NA
NAPEPLD	DEGs-DIABLO	NA		NA	NA	NA
NEU1	LF2_mods	NA		NA	NA	NA
NFIL3	DEGs-DIABLO-LF2	NA		NA	NA	NA
NFKBIA	DIABLO-LF2-mods		1	NA	NA	NA
NR1D2	DIABLO-LF2		1	NA	NA	NA
NR4A1	DEGs-DIABLO-LF2-Mods		1	NA	NA	NA
NR4A2	DEGs-DIABLO-LF2-Mods		1	NA	NA	NA
NUFIP2	LF2_mods		1	NA	NA	NA
OAT	LF2_mods	NA		NA	NA	NA
ODC1	DIABLO-LF2	NA		NA	NA	NA
OSM	DIABLO-LF2		1	NA	NA	NA
P2RY10	DIABLO-LF2	NA		NA	NA	NA
PER1	DIABLO-LF2		1	NA	NA	NA
PFKFB3	DIABLO-LF2		1	NA	NA	NA
PIGA	DIABLO-LF2	NA		NA	NA	NA
PIM3	DIABLO-LF2		1	NA	NA	NA
PLK2	LF2_mods	NA		NA	NA	NA
PMAIP1	DIABLO-LF2-mods		1	NA	NA	NA
PNP	LF2_mods	NA		NA	NA	NA
PNRC1	DIABLO-LF2-mods	NA		NA	NA	NA
POU3F1	LF2_mods	NA		NA	NA	NA
PRKCQ	DIABLO-LF2		1	NA	NA	NA
PTGER4	DIABLO-LF2-mods		1	NA	NA	NA
PTP4A1	DIABLO-LF2-mods	NA		NA	NA	NA
RAB33B	LF2_mods		1	NA	NA	NA
RNF139	DIABLO-LF2-mods	NA		NA	NA	NA
RNF19B	DIABLO-LF2-mods	NA		NA	NA	NA
SERTAD1	LF2_mods	NA		NA	NA	NA
SGK1	DIABLO-LF2-mods	NA		NA	NA	NA
SGMS1	DIABLO-LF2	NA		NA	NA	NA
SIAH2	DIABLO-LF2	NA		NA	NA	NA
SIK1	DEGs-DIABLO-LF2-Mods	NA		NA	NA	NA
SIRT1	LF2_mods	NA		NA	NA	NA
SLC1A5	LF2_mods		1	NA	NA	NA
SLC2A3	DIABLO-LF2-mods	NA		NA	NA	NA
SLC30A1	LF2_mods		1	NA	NA	NA
SLC35A1	DIABLO-LF2	NA		NA	NA	NA
SLC35A2	LF2_mods	NA		NA	NA	NA
SLC38A2	LF2_mods	NA		NA	NA	NA

SLC3A2	DIABLO-LF2	NA		NA	NA	NA
SMAD7	DEGs-DIABLO-LF2-Mods	NA		NA	NA	NA
SOCS1	LF2_mods		1	NA	NA	NA
SOCS3	LF2_mods		1	NA	NA	NA
SPTY2D1	DIABLO-LF2-mods		1	NA	NA	NA
SRGN	DIABLO-LF2		1	NA	NA	NA
TAF13	DIABLO-LF2	NA		NA	NA	NA
TFRC	DIABLO-LF2	NA		NA	NA	NA
TIPARP	DIABLO-LF2-mods		1	NA	NA	NA
TNFAIP3	DEGs-DIABLO-LF2-Mods		1	NA	NA	NA
TP53INP2	DEGs-DIABLO-LF2-Mods	NA		NA	NA	NA
TSC22D2	LF2_mods		1	NA	NA	NA
TUBA1A	DIABLO-LF2-mods	NA		NA	NA	NA
TUBA1B	LF2_mods	NA		NA	NA	NA
TUBA4A	LF2_mods	NA		NA	NA	NA
TUBB2A	DEGs-DIABLO-LF2-Mods	NA		NA	NA	NA
TUBB4B	LF2_mods	NA		NA	NA	NA
UBC	DIABLO-LF2		1	NA	1	NA
UBE2S	LF2_mods	NA		NA	NA	NA
XYLT1	DIABLO-LF2	NA		NA	NA	NA
YPEL5	DIABLO-LF2-mods	NA		NA	NA	NA
YRDC	DIABLO-LF2	NA		NA	NA	NA
ZFP36	DIABLO-LF2-mods	NA		NA	NA	NA
ZFP36L2	DIABLO-LF2-mods	NA		NA	NA	NA
ZNF331	DEGs-DIABLO-LF2		1	NA	NA	NA
ZNF622	DIABLO-LF2	NA		NA	NA	NA
ZNF703	LF2_mods	NA		NA	NA	NA

IBD susceptil eQTL		CD_OT_drug	UC_OT_drug	IBD_OT_druğ	PS_OT_drug	SC_OT_drug.
NA	NA	NA	NA	NA	NA	NA
NA	NA	NA	NA	NA	NA	NA
NA	NA	NA	NA	NA	NA	NA
NA	NA	NA	NA	NA	NA	NA
NA	NA	NA	NA	NA	NA	NA
1	NA	NA	NA	NA	NA	NA
NA	1	NA	NA	NA	NA	NA
NA	NA	NA	NA	NA	NA	NA
NA	NA	NA	NA	NA	NA	NA
NA	NA	NA	NA	NA	NA	NA
NA	NA	NA	NA	NA	NA	NA
NA	NA	NA	NA	NA	NA	NA
NA	1	NA	NA	NA	NA	NA
NA	NA	NA	NA	NA	NA	NA
NA	NA	NA	NA	NA	NA	NA
NA	NA	NA	NA	NA	NA	NA
NA	NA	NA	NA	NA	NA	NA
NA	NA	NA	NA	NA	NA	NA
1	NA	NA	NA	NA	NA	NA
NA	NA	NA	NA	1	NA	NA
NA	1	NA	NA	NA	NA	NA
NA	NA	NA	NA	NA	NA	NA
NA	NA	NA	NA	NA	NA	NA
NA	NA	NA	NA	NA	NA	NA
NA	NA	NA	NA	NA	NA	NA
NA	NA	NA	NA	NA	NA	NA
NA	NA	NA	NA	NA	NA	NA
NA	NA	NA	NA	NA	NA	NA
NA	NA	NA	NA	NA	NA	NA
NA	NA	NA	NA	NA	NA	NA
NA	NA	NA	NA	NA	NA	NA
NA	NA	NA	NA	NA	NA	NA
NA	NA	NA	NA	NA	NA	NA
NA	NA	NA	NA	NA	NA	NA
NA	1	NA	NA	NA	NA	NA
NA	NA	NA	NA	NA	NA	NA
1	NA	NA	NA	NA	NA	NA
NA	NA	NA	NA	NA	NA	NA
1	1	NA	NA	NA	NA	NA
NA	NA	NA	NA	NA	NA	NA
NA	NA	NA	NA	NA	NA	NA
NA	1	NA	NA	NA	NA	NA
NA	NA	NA	NA	NA	NA	NA
NA	NA	NA	NA	NA	NA	NA
NA	NA	NA	NA	NA	NA	NA
NA	NA	NA	NA	NA	NA	NA
1	NA	NA	NA	NA	NA	NA

NA	NA	NA	NA	NA	NA	NA
NA	NA	NA	NA	NA	NA	NA
NA	NA	NA	NA	NA	NA	NA
NA	NA	NA	NA	NA	NA	NA
NA	NA	NA	NA	NA	NA	NA
NA	NA	NA	NA	NA	NA	NA
NA	NA	NA	NA	NA	NA	NA
NA	NA	NA	NA	NA	NA	NA
NA	NA	NA	NA	NA	NA	NA
NA	NA	NA	NA	NA	NA	NA
NA	NA	NA	NA	NA	NA	NA
NA	NA	NA	NA	NA	NA	NA
NA	1	NA	NA	NA	NA	NA
NA	NA	NA	NA	NA	NA	NA
NA	NA	NA	NA	NA	NA	NA
NA	NA	NA	NA	NA	NA	NA
NA	NA	NA	NA	NA	NA	NA
NA	NA	NA	NA	NA	NA	NA
NA	NA	NA	NA	NA	NA	NA
NA	NA	NA	NA	NA	NA	NA
NA	NA	NA	NA	NA	NA	NA
NA	NA	NA	NA	NA	NA	NA
NA	NA	NA	NA	NA	NA	NA
NA	NA	NA	NA	NA	NA	NA
NA	NA	NA	NA	NA	NA	NA
NA	NA	NA	NA	NA	NA	NA
NA	NA	NA	NA	NA	NA	NA
NA	NA	NA	NA	NA	NA	NA
NA	NA	NA	NA	NA	NA	NA
NA	NA	NA	NA	NA	NA	NA
NA	NA	NA	NA	NA	NA	NA
NA	NA	NA	NA	NA	NA	NA
NA	NA	NA	NA	NA	NA	NA
NA	NA	NA	NA	NA	NA	NA
NA	NA	NA	NA	NA	NA	NA
NA	NA	NA	NA	NA	NA	NA
NA	NA	NA	NA	NA	NA	NA
NA	NA	NA	NA	NA	NA	NA
NA	NA	NA	NA	NA	NA	NA
NA	NA	NA	NA	NA	NA	NA
NA	NA	NA	NA	NA	NA	NA
NA	NA	NA	NA	NA	NA	NA
NA	NA	NA	NA	NA	NA	NA
NA	NA	NA	1	1	1	NA

NA	NA	NA	1	1	1	NA
NA	NA	NA	1	1	1	NA
NA	NA	NA	1	1	1	NA
NA	NA	NA	1	1	1	NA
NA	NA	NA	1	1	1	NA
NA	NA	NA	NA	NA	NA	NA
NA	NA	NA	NA	NA	NA	NA
NA	1	NA	NA	NA	NA	NA
NA	NA	NA	NA	NA	NA	NA
NA	NA	NA	NA	NA	NA	NA
NA	NA	NA	NA	NA	NA	NA
NA	NA	NA	NA	NA	NA	NA
NA	NA	NA	NA	NA	NA	NA
NA	1	NA	NA	NA	NA	NA
NA	NA	NA	NA	NA	NA	NA
NA	NA	NA	NA	NA	NA	NA
NA	1	NA	NA	NA	NA	NA
NA	NA	NA	NA	NA	NA	NA
NA	1	NA	NA	NA	NA	NA
NA	NA	NA	NA	NA	NA	NA
NA	NA	NA	NA	NA	NA	NA
NA	NA	NA	NA	NA	NA	NA
NA	NA	NA	NA	NA	NA	NA
NA	NA	NA	NA	NA	NA	NA
NA	NA	NA	NA	NA	NA	NA
NA	NA	NA	NA	NA	NA	NA
NA	NA	NA	NA	NA	NA	NA
NA	NA	NA	NA	NA	NA	NA
NA	NA	NA	NA	NA	NA	NA
NA	1	NA	NA	NA	NA	NA
NA	NA	NA	NA	NA	NA	NA
NA	NA	NA	NA	NA	NA	NA
1	NA	NA	1	1	1	NA
1	NA	NA	1	1	NA	NA
NA	NA	NA	NA	NA	NA	NA
NA	1	NA	NA	NA	NA	NA
NA	NA	NA	NA	NA	NA	NA
NA	NA	NA	NA	NA	NA	NA
NA	NA	NA	NA	NA	NA	NA
NA	NA	NA	NA	NA	NA	NA
NA	NA	NA	NA	NA	NA	NA
NA	NA	NA	NA	NA	NA	NA
NA	NA	NA	NA	NA	NA	NA
NA	NA	NA	1	1	1	NA
NA	NA	NA	NA	NA	NA	NA
NA	NA	NA	NA	NA	NA	NA
NA	1	NA	NA	NA	NA	NA
NA	NA	NA	NA	NA	NA	NA
NA	NA	NA	NA	NA	NA	NA

NA	NA	NA	NA	NA	NA	NA
NA	NA	1	1	1	NA	NA
1	NA	NA	NA	NA	NA	NA
NA	NA	NA	NA	NA	NA	NA
NA	1	NA	NA	NA	NA	NA
NA	NA	NA	NA	NA	NA	NA
NA	NA	NA	NA	NA	NA	NA
NA	NA	NA	NA	NA	NA	NA
NA	1	NA	NA	NA	NA	NA
1	NA	NA	NA	NA	NA	NA
NA	NA	NA	NA	NA	NA	NA
NA	1	NA	NA	NA	NA	NA
NA	NA	NA	NA	NA	NA	NA
NA	NA	NA	NA	NA	NA	NA
NA	NA	NA	NA	NA	NA	NA
NA	NA	NA	NA	NA	NA	NA
NA	NA	NA	NA	NA	1	NA
NA	NA	NA	NA	NA	1	NA
NA	NA	NA	NA	NA	NA	NA
NA	NA	NA	NA	NA	NA	NA
NA	NA	NA	NA	NA	NA	NA
NA	NA	NA	NA	NA	NA	NA
NA	NA	NA	NA	NA	NA	NA
NA	NA	NA	NA	NA	NA	NA
NA	1	NA	NA	NA	NA	NA
NA	NA	NA	NA	NA	NA	NA
NA	NA	NA	NA	NA	NA	NA

AS_OT_drug	RA_OT_drug	Druggability_1s	Druggability_2s	ADRs_TARD	DEG_FDR_0.1_log2FC_1
NA	NA	1	NA	NA	NA
NA	NA	1	NA	NA	NA
NA	NA	1	NA	NA	1
NA	NA	1	NA	NA	NA
NA	NA	1	NA	NA	NA
NA	NA	1	NA	NA	NA
NA	NA	1	NA	NA	NA
NA	NA	1	NA	NA	1
NA	NA	1	NA	NA	NA
NA	NA	1	NA	NA	NA
NA	NA	1	NA	NA	NA
NA	NA	1	NA	NA	NA
NA	NA	1	NA	NA	1
NA	NA	1	NA	NA	1
NA	NA	1	NA	NA	NA
NA	NA	1	NA	NA	NA
NA	NA	1	NA	NA	NA
NA	NA	1	NA	NA	NA
NA	NA	1	NA	NA	1
NA	NA	1	1	NA	NA
NA	NA	NA	NA	1	NA
NA	NA	1	NA	NA	NA
NA	NA	1	NA	NA	NA
NA	NA	1	NA	NA	NA
NA	NA	1	NA	NA	1
NA	NA	1	NA	NA	NA
NA	NA	1	NA	NA	NA
NA	NA	1	NA	NA	NA
NA	NA	1	NA	NA	NA
NA	NA	1	NA	NA	NA
NA	NA	1	NA	NA	1
NA	NA	1	NA	NA	1
NA	NA	1	NA	NA	NA
NA	NA	1	NA	NA	NA
NA	NA	1	NA	NA	NA
NA	NA	1	NA	NA	NA
NA	NA	1	NA	NA	NA
NA	NA	1	NA	NA	1
NA	NA	1	NA	NA	1
NA	NA	1	NA	NA	NA
NA	NA	1	NA	NA	NA
NA	NA	1	NA	NA	NA
NA	NA	1	NA	NA	NA
NA	NA	1	NA	NA	NA
NA	NA	1	NA	NA	NA
NA	NA	1	NA	NA	NA
NA	NA	1	NA	NA	NA
NA	NA	1	1	NA	NA

NA	NA	1	NA	NA	NA
NA	NA	1	NA	NA	1
NA	NA	1	NA	NA	NA
NA	NA	1	NA	NA	NA
NA	NA	1	NA	NA	NA
NA	NA	1	NA	NA	NA
NA	NA	1	NA	NA	NA
NA	NA	1	NA	NA	NA
NA	NA	1	NA	NA	NA
NA	NA	1	NA	NA	NA
NA	NA	1	NA	NA	NA
NA	NA	1	NA	NA	NA
NA	NA	1	NA	NA	NA
NA	NA	1	NA	NA	NA
NA	NA	1	NA	NA	NA
NA	NA	1	NA	NA	NA
NA	NA	1	NA	NA	NA
NA	NA	1	NA	NA	NA
NA	NA	1	NA	NA	NA
NA	NA	1	NA	NA	NA
NA	NA	1	NA	NA	NA
NA	NA	1	NA	NA	NA
NA	NA	1	NA	NA	NA
NA	NA	1	NA	NA	NA
NA	NA	1	NA	NA	NA
NA	NA	1	NA	NA	NA
NA	NA	1	NA	NA	NA
NA	NA	1	NA	NA	NA
NA	NA	1	NA	NA	NA
NA	NA	1	NA	NA	NA
NA	NA	1	NA	NA	NA
NA	NA	1	NA	NA	NA
NA	NA	1	NA	NA	NA
NA	NA	1	NA	NA	NA
NA	NA	1	NA	NA	NA
NA	NA	1	NA	NA	NA
NA	NA	1	NA	NA	NA
NA	NA	1	NA	NA	NA
NA	NA	1	NA	NA	NA
NA	NA	1	NA	NA	NA
NA	NA	1	NA	NA	NA
NA	1	1	1	NA	NA

NA	1	1	1	NA	NA
NA	1	1	1	NA	NA
NA	1	1	1	NA	NA
NA	1	1	1	NA	NA
NA	1	1	1	NA	NA
NA	NA	1	NA	NA	NA
NA	NA	1	NA	NA	NA
NA	NA	1	NA	NA	NA
NA	NA	1	NA	NA	NA
NA	NA	1	NA	NA	1
NA	NA	1	NA	NA	NA
NA	NA	1	NA	NA	1
NA	NA	1	1	NA	NA
NA	NA	1	NA	NA	1
NA	NA	1	NA	NA	1
NA	NA	NA	NA	NA	NA
NA	NA	1	NA	NA	NA
NA	NA	1	NA	1	NA
NA	NA	1	NA	NA	NA
NA	NA	1	NA	NA	NA
NA	NA	1	NA	NA	NA
NA	NA	1	NA	NA	NA
NA	NA	1	NA	NA	NA
NA	NA	1	NA	NA	NA
NA	NA	1	NA	NA	NA
NA	NA	1	NA	NA	NA
NA	NA	1	NA	NA	NA
NA	NA	1	NA	NA	NA
NA	NA	1	1	NA	NA
NA	1	1	1	1	NA
NA	NA	1	NA	NA	NA
NA	NA	1	NA	NA	NA
NA	NA	1	NA	NA	NA
NA	NA	1	NA	NA	NA
NA	NA	1	NA	NA	NA
NA	NA	1	NA	NA	NA
NA	NA	1	NA	NA	NA
NA	NA	1	NA	NA	NA
NA	NA	1	NA	NA	1
NA	NA	1	1	1	NA
NA	NA	1	NA	NA	NA
NA	NA	1	NA	NA	NA
NA	NA	1	NA	NA	NA
NA	NA	1	1	NA	NA
NA	NA	1	NA	NA	NA
NA	NA	1	NA	NA	NA
NA	NA	1	NA	NA	NA

NA	NA	1	NA	NA	NA
NA	NA	1	NA	NA	1
NA	NA	1	1	NA	NA
NA	NA	1	NA	NA	NA
NA	NA	NA	NA	NA	NA
NA	NA	1	NA	NA	NA
NA	NA	1	NA	NA	NA
NA	NA	1	NA	NA	NA
NA	NA	1	NA	NA	NA
NA	NA	1	1	NA	1
NA	NA	1	NA	NA	1
NA	NA	NA	NA	NA	NA
NA	NA	1	NA	NA	NA
NA	NA	1	NA	NA	NA
NA	NA	1	NA	NA	NA
NA	1	1	NA	NA	1
NA	1	1	NA	NA	NA
NA	NA	1	NA	NA	NA
NA	NA	1	NA	NA	NA
NA	NA	1	NA	NA	NA
NA	NA	1	NA	NA	NA
NA	NA	1	NA	NA	NA
NA	NA	1	NA	NA	NA
NA	NA	1	NA	NA	NA
NA	NA	1	NA	NA	1
NA	NA	1	NA	NA	NA
NA	NA	1	NA	NA	NA

DEG_FDR_0.1_log2FC_0.5	UC vs L1 (UP/DOWN-regulation)	log2FC	IBD_path
1	DOWN	-0,8645643	0
NA	DOWN	-0,3232243	0
1	DOWN	-1,3986805	0
NA	DOWN	-0,2443773	0
1	DOWN	-0,9052901	0
NA	DOWN	-0,4722703	1
NA	DOWN	-0,2215873	1
1	DOWN	-1,1227267	0
NA	UP	0,05587804	0
NA	DOWN	-0,2257226	0
NA	DOWN	-0,365957	0
1	DOWN	-0,6636222	0
1	DOWN	-0,5867451	0
1	DOWN	-1,4781731	1
1	DOWN	-2,020562	0
1	DOWN	-0,5454792	0
NA	DOWN	-0,1403614	0
NA	DOWN	-0,4168107	0
NA	DOWN	-0,2647741	0
1	DOWN	-1,0725734	1
NA	DOWN	-0,4232301	1
1	DOWN	-0,5241672	1
NA	DOWN	-0,5505859	0
1	DOWN	-0,5837984	0
NA	DOWN	-0,4177612	0
1	DOWN	-1,0496186	0
1	DOWN	-0,7890283	0
1	DOWN	-0,9120287	0
1	DOWN	-0,814372	0
1	DOWN	-0,9827876	0
NA	DOWN	-0,1475331	0
1	DOWN	-1,3983796	0
1	DOWN	-1,3832812	0
NA	DOWN	-0,4309784	0
NA	DOWN	-0,255991	1
NA	DOWN	-0,732489	0
NA	DOWN	-0,5808991	1
NA	DOWN	-0,633634	0
1	DOWN	-1,3073953	1
NA	DOWN	-0,6915638	0
NA	DOWN	-0,5652356	0
NA	DOWN	-0,4204348	1
1	DOWN	-0,7990049	0
NA	DOWN	-0,3284407	0
NA	DOWN	-0,5295784	0
1	DOWN	-0,6166111	0
1	DOWN	-0,6457591	1

NA	DOWN	-0,4498437	0
1	DOWN	-1,3008274	0
NA	DOWN	-0,2821408	0
NA	DOWN	-0,6758139	0
NA	DOWN	-0,6488319	0
1	DOWN	-0,5040753	0
NA	DOWN	-0,1630578	0
NA	DOWN	-0,1849143	0
NA	DOWN	-1,0623889	0
NA	DOWN	-0,4185714	0
NA	UP	0,12756149	0
NA	DOWN	-0,4502897	0
NA	DOWN	-0,2811757	0
NA	DOWN	-0,4969255	0
1	DOWN	-0,5603043	1
NA	DOWN	-0,4094846	0
NA	DOWN	-0,3052449	0
1	DOWN	-0,7655747	0
NA	DOWN	-0,4794424	0
NA	DOWN	-0,5013862	0
NA	DOWN	-0,4705435	0
1	DOWN	-0,628667	0
NA	DOWN	-0,2839779	0
NA	DOWN	-0,222066	0
1	DOWN	-0,9007233	0
1	DOWN	-0,6244434	0
1	DOWN	-0,6137376	0
NA	DOWN	-0,3069521	1
1	DOWN	-1,7831689	0
1	DOWN	-0,6679578	1
1	DOWN	-0,6567398	0
NA	DOWN	-0,3599633	0
1	DOWN	-0,5337514	0
NA	DOWN	-0,7150591	0
NA	UP	0,11262509	0
NA	DOWN	-0,4290521	0
NA	UP	0,34663494	1
1	DOWN	-1,1912799	0
1	DOWN	-0,6427097	0
NA	DOWN	-0,2295067	0
NA	UP	0,07272971	0
NA	UP	0,21855993	0
NA	DOWN	-0,4049286	0
NA	UP	0,09486707	0
NA	UP	0,07064231	0
NA	UP	0,0275914	0
NA	UP	0,10709593	0
NA	UP	0,09074788	0

NA	UP	0,08623284	0
NA	UP	0,08682953	0
NA	UP	0,2015388	0
NA	UP	0,16463293	0
NA	UP	0,00445984	0
NA	DOWN	-0,0303424	0
NA	DOWN	-0,4878941	0
NA	DOWN	-0,3263268	1
1	DOWN	-0,9717678	0
1	UP	1,08974958	0
1	DOWN	-0,7825998	0
1	DOWN	-1,0548635	0
1	DOWN	-0,6581822	0
NA	DOWN	-0,3853246	1
1	DOWN	-1,3830236	0
1	DOWN	-1,0348639	0
NA	DOWN	-0,1022137	1
NA	DOWN	-0,3016626	0
NA	DOWN	-0,4655042	0
1	DOWN	-0,7751732	0
1	DOWN	-0,5132971	0
1	DOWN	-0,7722103	0
1	DOWN	-0,8207638	0
NA	DOWN	-0,4861513	0
1	DOWN	-0,6590407	0
NA	DOWN	-0,2747099	0
NA	DOWN	-0,7362575	1
NA	DOWN	-0,1402062	0
NA	DOWN	-0,3508827	0
NA	DOWN	-0,4197085	0
NA	DOWN	-0,2663772	1
1	DOWN	-0,9236738	1
1	DOWN	-0,6480574	0
NA	DOWN	-0,3062933	1
NA	DOWN	-0,3742072	0
1	DOWN	-0,6222355	0
NA	DOWN	-0,3395818	0
1	DOWN	-0,8478855	0
NA	DOWN	-0,4078453	0
NA	DOWN	-0,4704996	0
1	DOWN	-1,0293169	0
NA	DOWN	-0,3122223	0
NA	DOWN	-0,6410879	0
1	DOWN	-0,9740432	0
NA	DOWN	-0,258694	1
1	UP	0,82058971	0
NA	DOWN	-0,1651374	0
NA	DOWN	-0,3272159	0

NA	DOWN	-0,2602121	0
1	DOWN	-1,1660793	0
NA	DOWN	-0,2524845	1
1	DOWN	-0,5480009	0
1	DOWN	-0,5595209	1
1	DOWN	-0,7769913	0
1	DOWN	-0,6716295	0
NA	DOWN	-0,3775501	0
1	DOWN	-0,571003	1
1	DOWN	-1,0621379	1
1	DOWN	-1,2359345	0
1	DOWN	-0,5351233	1
NA	DOWN	-0,4667487	0
NA	DOWN	-0,1783176	0
NA	DOWN	-0,2692345	0
1	DOWN	-1,0047516	0
NA	DOWN	-0,4198666	0
NA	DOWN	-0,3728648	1
NA	DOWN	-0,578054	0
NA	DOWN	-0,3667091	0
1	DOWN	-0,7822234	0
NA	DOWN	-0,3761356	0
1	DOWN	-0,9274354	0
NA	DOWN	-0,3724031	0
1	DOWN	-1,1756283	1
NA	DOWN	-0,322366	0
NA	DOWN	-0,8311596	0

IBD_DT	nonIBD_DT	UC_meta_ar	UC_meta_ar	UC_meta_ar	hubinfo
0	0	NA	NA	NA	mod1_hub1
0	0	NA	NA	NA	NA
0	0	NA	NA	NA	NA
0	0	NA	NA	NA	NA
0	0	NA	NA	NA	NA
0	0	NA	NA	NA	NA
0	0	NA	NA	NA	NA
0	0	NA	NA	NA	NA
0	0	1	0,91164884	8	NA
0	0	NA	NA	NA	NA
0	0	NA	NA	NA	mod2_hub7
0	0	NA	NA	NA	NA
0	0	NA	NA	NA	NA
0	0	NA	NA	NA	NA
0	0	NA	NA	NA	NA
0	0	NA	NA	NA	NA
0	0	NA	NA	NA	NA
0	0	NA	NA	NA	NA
0	0	NA	NA	NA	NA
0	0	NA	NA	NA	NA
0	0	NA	NA	NA	NA
1	0	1	0,84894777	8	NA
0	0	1	-0,8086539	8	NA
0	0	NA	NA	NA	NA
0	0	NA	NA	NA	mod2_hub8
0	0	NA	NA	NA	NA
0	0	1	0,71408021	8	NA
0	0	NA	NA	NA	NA
0	0	1	0,892603	6	NA
0	0	NA	NA	NA	NA
0	0	NA	NA	NA	NA
0	0	NA	NA	NA	NA
0	0	NA	NA	NA	NA
0	0	NA	NA	NA	NA
0	0	NA	NA	NA	mod2_hub9
0	0	NA	NA	NA	NA
0	0	1	0,62314919	8	NA
0	0	NA	NA	NA	NA
0	0	NA	NA	NA	mod1_hub4
0	0	NA	NA	NA	NA
0	0	NA	NA	NA	NA
0	0	NA	NA	NA	NA
0	0	NA	NA	NA	NA
0	0	NA	NA	NA	NA
0	0	NA	NA	NA	NA
0	0	NA	NA	NA	NA
0	0	NA	NA	NA	NA
0	0	1	0,93888835	8	NA

0	0 NA	NA	NA	NA
0	0 NA	NA	NA	NA
0	0 NA	NA	NA	NA
0	0 NA	NA	NA	NA
0	0 NA	NA	NA	mod2_hub13
0	0 NA	NA	NA	NA
0	0 NA	NA	NA	NA
0	0 NA	NA	NA	NA
0	0 NA	NA	NA	NA
0	0 NA	NA	NA	NA
0	0 NA	NA	NA	NA
0	0 NA	NA	NA	NA
0	0 NA	NA	NA	NA
0	0 NA	NA	NA	NA
0	0 NA	NA	NA	NA
0	0	1 0,85190899		8 NA
0	0 NA	NA	NA	NA
0	0 NA	NA	NA	NA
0	0 NA	NA	NA	NA
0	0 NA	NA	NA	mod1_hub6
0	0 NA	NA	NA	NA
0	0 NA	NA	NA	NA
0	0 NA	NA	NA	NA
0	0 NA	NA	NA	NA
0	0 NA	NA	NA	NA
0	0 NA	NA	NA	NA
0	0 NA	NA	NA	NA
0	0	1 0,69777705		8 NA
0	0 NA	NA	NA	NA
0	0 NA	NA	NA	NA
0	0 NA	NA	NA	NA
0	0 NA	NA	NA	NA
0	0 NA	NA	NA	NA
0	0 NA	NA	NA	NA
0	0	1 0,78973256		8 NA
0	0 NA	NA	NA	NA
0	0 NA	NA	NA	NA
0	0 NA	NA	NA	NA
0	0	1 0,59597121		8 NA
0	0 NA	NA	NA	mod2_hub10
0	0 NA	NA	NA	NA
0	0 NA	NA	NA	NA
0	0 NA	NA	NA	mod2_hub14
0	0 NA	NA	NA	NA
0	0 NA	NA	NA	NA
0	0 NA	NA	NA	NA
1	1 NA	NA	NA	NA

1	1 NA	NA	NA	NA
1	1 NA	NA	NA	NA
1	1 NA	NA	NA	NA
1	1 NA	NA	NA	NA
1	1 NA	NA	NA	NA
0	0 NA	NA	NA	NA
0	0 NA	NA	NA	NA
0	0	1 -0,5951815		8 NA
0	0	1 1,03864802		8 NA
0	0	1 -0,6258896		8 NA
0	0 NA	NA	NA	NA
0	0 NA	NA	NA	NA
0	0 NA	NA	NA	NA
0	0 NA	NA	NA	NA
0	0 NA	NA	NA	NA
0	0	1 0,69436444		8 mod1_hub9
0	0 NA	NA	NA	NA
0	0 NA	NA	NA	NA
0	0 NA	NA	NA	NA
0	0	1 0,65139435		8 NA
0	0 NA	NA	NA	NA
0	0 NA	NA	NA	NA
0	0	1 1,4027006		8 NA
0	0 NA	NA	NA	NA
0	0	1 0,73063703		8 NA
0	0 NA	NA	NA	mod2_hub4
0	0 NA	NA	NA	NA
0	0 NA	NA	NA	NA
0	0 NA	NA	NA	NA
0	0 NA	NA	NA	NA
0	0 NA	NA	NA	NA
0	0 NA	NA	NA	mod2_hub2
0	0 NA	NA	NA	NA
0	0	1 0,71190829		6 NA
0	0 NA	NA	NA	NA
0	0 NA	NA	NA	mod1_hub8
1	1 NA	NA	NA	NA
0	0 NA	NA	NA	NA
0	0	1 1,32549545		8 mod1_hub7
0	0 NA	NA	NA	NA
0	0 NA	NA	NA	NA
0	0 NA	NA	NA	NA
0	0 NA	NA	NA	NA

0	0 NA	NA	NA	NA
1	0 NA	NA	NA	NA
0	0	1 1,22904468		8 NA
0	0	1 1,65013306		8 NA
0	0 NA	NA	NA	NA
0	0	1 1,36074948		8 NA
0	0 NA	NA	NA	NA
0	0 NA	NA	NA	NA
0	0 NA	NA	NA	NA
0	0 NA	NA	NA	NA
0	0	1 -0,6344073		8 NA
0	0 NA	NA	NA	NA
0	0 NA	NA	NA	mod1_hub2
0	0 NA	NA	NA	NA
0	0 NA	NA	NA	NA
0	1 NA	NA	NA	NA
0	1 NA	NA	NA	mod2_hub1
0	0 NA	NA	NA	NA
0	0 NA	NA	NA	NA
0	0 NA	NA	NA	NA
0	0 NA	NA	NA	NA
0	0 NA	NA	NA	mod1_hub5
0	0 NA	NA	NA	NA
0	0 NA	NA	NA	NA
0	0 NA	NA	NA	NA
0	0 NA	NA	NA	NA

Rank	1-cos(α)	Perturbation Compound_Summary	Cell-line
1	18.303	STK397047 http://pubchem.ncbi.nlm.nih.gov/compound/STK397047	A375
2	18.301	Chemistry http://life.ccs.miami.edu/life/sumn	SW620
3	18.293	BRD-A36630 http://pubchem.ncbi.nlm.nih.gov/compound/BRD-A36630	SKLU1
4	18.261	BRD-K92317 http://pubchem.ncbi.nlm.nih.gov/compound/BRD-K92317	PL21
5	18.196	PubChem C1C http://pubchem.ncbi.nlm.nih.gov/compound/C1C	VCAP
6	18.157	withaferin-a http://pubchem.ncbi.nlm.nih.gov/compound/withaferin-a	SKBR3
7	18.153	BRD-K04853 http://pubchem.ncbi.nlm.nih.gov/compound/BRD-K04853	HT29
8	18.130	PubChem C1C http://pubchem.ncbi.nlm.nih.gov/compound/C1C	VCAP
9	18.121	celastrol http://pubchem.ncbi.nlm.nih.gov/compound/celastrol	HS578T
10	18.102	BRD-K04853 http://pubchem.ncbi.nlm.nih.gov/compound/BRD-K04853	HT29
11	18.102	Narciclasine http://pubchem.ncbi.nlm.nih.gov/compound/Narciclasine	HCC15
12	18.102	BRD-K92317 http://pubchem.ncbi.nlm.nih.gov/compound/BRD-K92317	HCC515
13	18.093	BRD-K28916 http://pubchem.ncbi.nlm.nih.gov/compound/BRD-K28916	A549
14	18.069	Ryuvidine http://pubchem.ncbi.nlm.nih.gov/compound/Ryuvidine	HCC515
15	18.066	withaferin-a http://pubchem.ncbi.nlm.nih.gov/compound/withaferin-a	BT20
16	18.057	withaferin-a http://pubchem.ncbi.nlm.nih.gov/compound/withaferin-a	SKBR3
17	18.055	F1566-0341 http://pubchem.ncbi.nlm.nih.gov/compound/F1566-0341	HT29
18	18.052	7241-4207 http://pubchem.ncbi.nlm.nih.gov/compound/7241-4207	VCAP
19	18.039	STK249718 http://pubchem.ncbi.nlm.nih.gov/compound/STK249718	HCC515
20	18.030	BRD-K98824 http://pubchem.ncbi.nlm.nih.gov/compound/BRD-K98824	A375
21	18.028	F1566-0341 http://pubchem.ncbi.nlm.nih.gov/compound/F1566-0341	VCAP
22	18.011	7241-4207 http://pubchem.ncbi.nlm.nih.gov/compound/7241-4207	HT29
23	17.994	BRD-K77877 http://pubchem.ncbi.nlm.nih.gov/compound/BRD-K77877	VCAP
24	17.994	BRD-K92317 http://pubchem.ncbi.nlm.nih.gov/compound/BRD-K92317	A375
25	17.979	F1566-0341 http://pubchem.ncbi.nlm.nih.gov/compound/F1566-0341	MCF7
26	17.971	celastrol http://pubchem.ncbi.nlm.nih.gov/compound/celastrol	BT20
27	17.960	BRD-K92317 http://pubchem.ncbi.nlm.nih.gov/compound/BRD-K92317	RMUGS
28	17.950	B4313 http://pubchem.ncbi.nlm.nih.gov/compound/B4313	VCAP
29	17.946	BRD-K80786 http://pubchem.ncbi.nlm.nih.gov/compound/BRD-K80786	HT29
30	17.942	BRD-K28907 http://pubchem.ncbi.nlm.nih.gov/compound/BRD-K28907	HCC15
31	17.934	Narciclasine http://pubchem.ncbi.nlm.nih.gov/compound/Narciclasine	T3M10
32	17.933	BRD-K68143 http://pubchem.ncbi.nlm.nih.gov/compound/BRD-K68143	HEPG2
33	17.928	TENIPOSIDE http://pubchem.ncbi.nlm.nih.gov/compound/TENIPOSIDE	SKLU1
34	17.924	YM-155 http://pubchem.ncbi.nlm.nih.gov/compound/YM-155	SW620
35	17.923	BRD-K91370 http://pubchem.ncbi.nlm.nih.gov/compound/BRD-K91370	HT29
36	17.921	BRD-K99633 http://pubchem.ncbi.nlm.nih.gov/compound/BRD-K99633	PC3
37	17.911	Narciclasine http://pubchem.ncbi.nlm.nih.gov/compound/Narciclasine	SKLU1
38	17.904	QL-XII-47 http://pubchem.ncbi.nlm.nih.gov/compound/QL-XII-47	HME1
39	17.888	VU0410183 http://pubchem.ncbi.nlm.nih.gov/compound/VU0410183	A375
40	17.885	celastrol http://pubchem.ncbi.nlm.nih.gov/compound/celastrol	MDAMB231
41	17.876	withaferin-a http://pubchem.ncbi.nlm.nih.gov/compound/withaferin-a	BT20
42	17.875	NCGC001885 http://pubchem.ncbi.nlm.nih.gov/compound/NCGC001885	VCAP
43	17.874	LDN-193189 http://pubchem.ncbi.nlm.nih.gov/compound/LDN-193189	HT29
44	17.867	BRD-K28916 http://pubchem.ncbi.nlm.nih.gov/compound/BRD-K28916	A375
45	17.864	curcumin http://pubchem.ncbi.nlm.nih.gov/compound/curcumin	HT29
46	17.864	BRD-K17140 http://pubchem.ncbi.nlm.nih.gov/compound/BRD-K17140	A673
47	17.862	mocetinosta http://pubchem.ncbi.nlm.nih.gov/compound/mocetinosta	A375

48 17.850 BRD-K996331 <http://pubchem.ncbi.nlm.nih.gov/compound/17850> HT29
49 17.839 mocetinostatin <http://pubchem.ncbi.nlm.nih.gov/compound/17839> PC3
50 17.836 YM-155 <http://pubchem.ncbi.nlm.nih.gov/compound/17836> A375

Dose	Time	URL
10.0um	6.0h	https://maayanlab.cloud/L1000CDS2/meta?sig_id=CPC014_A375_
10.0um	6.0h	https://maayanlab.cloud/L1000CDS2/meta?sig_id=CPC006_SW62
0.35um	6.0h	https://maayanlab.cloud/L1000CDS2/meta?sig_id=CPC006_SKLU1
10.0um	6.0h	https://maayanlab.cloud/L1000CDS2/meta?sig_id=CPC006_PL21_
10.0um	24.0h	https://maayanlab.cloud/L1000CDS2/meta?sig_id=CPC014_VCAP_
3.33um	24h	https://maayanlab.cloud/L1000CDS2/meta?sig_id=LJP005_SKBR3
10.0um	6.0h	https://maayanlab.cloud/L1000CDS2/meta?sig_id=CPC006_HT29_
10.0um	6.0h	https://maayanlab.cloud/L1000CDS2/meta?sig_id=CPC013_VCAP_
3.33um	24h	https://maayanlab.cloud/L1000CDS2/meta?sig_id=LJP006_HS578
10.0um	24.0h	https://maayanlab.cloud/L1000CDS2/meta?sig_id=CPC006_HT29_
10.0um	6.0h	https://maayanlab.cloud/L1000CDS2/meta?sig_id=CPC006_HCC15
10.0um	6.0h	https://maayanlab.cloud/L1000CDS2/meta?sig_id=CPC010_HCC51
10.0um	6.0h	https://maayanlab.cloud/L1000CDS2/meta?sig_id=CPC010_A549_
10.0um	6.0h	https://maayanlab.cloud/L1000CDS2/meta?sig_id=CPC001_HCC51
3.33um	24h	https://maayanlab.cloud/L1000CDS2/meta?sig_id=LJP005_BT20_
3.33um	24h	https://maayanlab.cloud/L1000CDS2/meta?sig_id=LJP006_SKBR3
10.0um	6.0h	https://maayanlab.cloud/L1000CDS2/meta?sig_id=CPC014_HT29_
10.0um	24.0h	https://maayanlab.cloud/L1000CDS2/meta?sig_id=CPC013_VCAP_
10.0um	6.0h	https://maayanlab.cloud/L1000CDS2/meta?sig_id=CPC014_HCC51
10.0um	6.0h	https://maayanlab.cloud/L1000CDS2/meta?sig_id=CPC019_A375_
10.0um	6.0h	https://maayanlab.cloud/L1000CDS2/meta?sig_id=CPC014_VCAP_
10.0um	6.0h	https://maayanlab.cloud/L1000CDS2/meta?sig_id=CPC013_HT29_
10.0um	24.0h	https://maayanlab.cloud/L1000CDS2/meta?sig_id=CPC020_VCAP_
10.0um	6.0h	https://maayanlab.cloud/L1000CDS2/meta?sig_id=CPC006_A375_
10.0um	6.0h	https://maayanlab.cloud/L1000CDS2/meta?sig_id=CPC014_MCF7
3.33um	24h	https://maayanlab.cloud/L1000CDS2/meta?sig_id=LJP006_BT20_
10.0um	6.0h	https://maayanlab.cloud/L1000CDS2/meta?sig_id=CPC006_RMUC
10.0um	24.0h	https://maayanlab.cloud/L1000CDS2/meta?sig_id=CPC014_VCAP_
10.0um	6.0h	https://maayanlab.cloud/L1000CDS2/meta?sig_id=CPC013_HT29_
11.1um	6.0h	https://maayanlab.cloud/L1000CDS2/meta?sig_id=CPC006_HCC15
10.0um	6.0h	https://maayanlab.cloud/L1000CDS2/meta?sig_id=CPC006_T3M1
10.0um	6.0h	https://maayanlab.cloud/L1000CDS2/meta?sig_id=CPC006_HEPG
1.25um	6.0h	https://maayanlab.cloud/L1000CDS2/meta?sig_id=CPC006_SKLU1
0.31um	6.0h	https://maayanlab.cloud/L1000CDS2/meta?sig_id=CPC006_SW62
10.0um	6.0h	https://maayanlab.cloud/L1000CDS2/meta?sig_id=CPC016_HT29_
10.0um	6.0h	https://maayanlab.cloud/L1000CDS2/meta?sig_id=CPC010_PC3_6
10.0um	6.0h	https://maayanlab.cloud/L1000CDS2/meta?sig_id=CPC006_SKLU1
3.33um	3h	https://maayanlab.cloud/L1000CDS2/meta?sig_id=LJP006_HME1_
10.0um	24.0h	https://maayanlab.cloud/L1000CDS2/meta?sig_id=CPC008_A375_
3.33um	24h	https://maayanlab.cloud/L1000CDS2/meta?sig_id=LJP006_MDAM
3.33um	24h	https://maayanlab.cloud/L1000CDS2/meta?sig_id=LJP006_BT20_
10.0um	6.0h	https://maayanlab.cloud/L1000CDS2/meta?sig_id=CPC007_VCAP_
10um	24h	https://maayanlab.cloud/L1000CDS2/meta?sig_id=LJP005_HT29_
10.0um	6.0h	https://maayanlab.cloud/L1000CDS2/meta?sig_id=CPC010_A375_
48.0um	24.0h	https://maayanlab.cloud/L1000CDS2/meta?sig_id=CPC006_HT29_
11.1um	6.0h	https://maayanlab.cloud/L1000CDS2/meta?sig_id=CPC006_A673_
10um	24h	https://maayanlab.cloud/L1000CDS2/meta?sig_id=LJP008_A375_

10.0um	6.0h	https://maayanlab.cloud/L1000CDS2/meta?sig_id=CPC010_HT29_
10um	24h	https://maayanlab.cloud/L1000CDS2/meta?sig_id=LJP008_PC3_2
0.31um	24.0h	https://maayanlab.cloud/L1000CDS2/meta?sig_id=CPC006_A375_

_6H:BRD-K80622725:10.0
0_6H:BRD-K74402642:10.0
L_6H:BRD-A36630025:0.35
6H:BRD-K92317137:10.0
_24H:BRD-A52193669:10.0
_24H:BRD-K88378636:3.33
_6H:BRD-K04853698:10.0
_6H:BRD-K69852452:10.0
T_24H:BRD-A24396574:3.33
_24H:BRD-K04853698:10.0
i_6H:BRD-K06792661:10.0
L5_6H:BRD-K92317137:10.0
_6H:BRD-K28916077:10.0
L5_6H:BRD-K06426971:10.0
24H:BRD-K88378636:3.33
_24H:BRD-K88378636:3.33
_6H:BRD-K69852452:10.0
_24H:BRD-K69852452:10.0
L5_6H:BRD-K81142122:10.0
_6H:BRD-K98824517:10.0
_6H:BRD-K69852452:10.0
_6H:BRD-K69852452:10.0
_24H:BRD-K77877933:10.0
_6H:BRD-K92317137:10.0
_6H:BRD-K69852452:10.0
24H:BRD-A24396574:3.33
iS_6H:BRD-K92317137:10.0
_24H:BRD-A11007541:10.0
_6H:BRD-K80786583:10.0
i_6H:BRD-K28907958:11.1
0_6H:BRD-K06792661:10.0
2_6H:BRD-K68143200:10.0
L_6H:BRD-A35588707:1.25
0_6H:BRD-K76703230:0.31
_6H:BRD-K91370081:10.0
iH:BRD-K99633092:10.0
L_6H:BRD-K06792661:10.0
_3H:BRD-K99252563:3.33
_24H:BRD-K74710236:10.0
IB231_24H:BRD-A24396574:3.33
24H:BRD-K88378636:3.33
_6H:BRD-A09719808:10.0
24H:BRD-K04853698:10
_6H:BRD-K28916077:10.0
_24H:BRD-K74148702:48.0
_6H:BRD-K17140735:11.1
24H:BRD-K16485616:10

_6H:BRD-K99633092:10.0

4H:BRD-K16485616:10

_24H:BRD-K76703230:0.31

Rank	1-cos(α)	Perturbation
1	0.2305	BMS-387032
2	0.2490	A443654
3	0.2540	JNK-9L
4	0.2558	alvocidib
5	0.2559	A443654
6	0.2561	PF-562271
7	0.2578	AT-7519
8	0.2630	alvocidib
9	0.2684	linifanib
10	0.2706	alvocidib
11	0.2777	A443654
12	0.2786	alvocidib
13	0.2803	CGP-60474
14	0.2808	A443654
15	0.2832	pelitinib
16	0.2838	CGP-60474
17	0.2846	CGP-60474
18	0.2860	AS-601245
19	0.2862	CGP-60474
20	0.2865	BMS-387032
21	0.2894	alvocidib
22	0.2933	CGP-60474
23	0.2949	alvocidib
24	0.2960	alvocidib
25	0.2972	PHA-793887
26	0.2980	16-HYDROXY
27	0.2985	AZD-5438
28	0.3001	daunorubicin
29	0.3050	alvocidib
30	0.3075	AT-7519
31	0.3084	BMS-387032
32	0.3087	alvocidib
33	0.3088	AT-7519
34	0.3097	alvocidib
35	0.3102	BMS-387032
36	0.3139	CGP-60474
37	0.3148	alvocidib
38	0.3152	JNK-9L
39	0.3156	CGP-60474
40	0.3168	JNK-9L
41	0.3183	JNK-9L
42	0.3191	CGP-60474
43	0.3205	CGP-60474
44	0.3208	A443654
45	0.3220	AT-7519
46	0.3223	CGP-60474
47	0.3232	AT-7519

48 0.3239A443654

49 0.3245CGP-60474

50 0.3251BMS-387032

Compound_Summary

<http://pubchem.ncbi.nlm.nih.gov/summary/summary.cgi?cid=3025986>
None
<http://pubchem.ncbi.nlm.nih.gov/summary/summary.cgi?cid=59588070>
<http://pubchem.ncbi.nlm.nih.gov/summary/summary.cgi?cid=5287969>
None
<http://pubchem.ncbi.nlm.nih.gov/summary/summary.cgi?cid=11713159>
<http://pubchem.ncbi.nlm.nih.gov/summary/summary.cgi?cid=11338033>
<http://pubchem.ncbi.nlm.nih.gov/summary/summary.cgi?cid=5287969>
<http://pubchem.ncbi.nlm.nih.gov/summary/summary.cgi?cid=11485656>
<http://pubchem.ncbi.nlm.nih.gov/summary/summary.cgi?cid=5287969>
None
<http://pubchem.ncbi.nlm.nih.gov/summary/summary.cgi?cid=5287969>
<http://pubchem.ncbi.nlm.nih.gov/summary/summary.cgi?cid=644215>
None
<http://pubchem.ncbi.nlm.nih.gov/summary/summary.cgi?cid=6445562>
<http://pubchem.ncbi.nlm.nih.gov/summary/summary.cgi?cid=644215>
<http://pubchem.ncbi.nlm.nih.gov/summary/summary.cgi?cid=644215>
<http://pubchem.ncbi.nlm.nih.gov/summary/summary.cgi?cid=10109823>
<http://pubchem.ncbi.nlm.nih.gov/summary/summary.cgi?cid=644215>
<http://pubchem.ncbi.nlm.nih.gov/summary/summary.cgi?cid=3025986>
<http://pubchem.ncbi.nlm.nih.gov/summary/summary.cgi?cid=5287969>
<http://pubchem.ncbi.nlm.nih.gov/summary/summary.cgi?cid=644215>
<http://pubchem.ncbi.nlm.nih.gov/summary/summary.cgi?cid=5287969>
<http://pubchem.ncbi.nlm.nih.gov/summary/summary.cgi?cid=5287969>
<http://pubchem.ncbi.nlm.nih.gov/summary/summary.cgi?cid=46191454>
<http://pubchem.ncbi.nlm.nih.gov/summary/summary.cgi?cid=16220015>
<http://pubchem.ncbi.nlm.nih.gov/summary/summary.cgi?cid=16747683>
<http://pubchem.ncbi.nlm.nih.gov/summary/summary.cgi?cid=3085107>
<http://pubchem.ncbi.nlm.nih.gov/summary/summary.cgi?cid=5287969>
<http://pubchem.ncbi.nlm.nih.gov/summary/summary.cgi?cid=11338033>
<http://pubchem.ncbi.nlm.nih.gov/summary/summary.cgi?cid=3025986>
<http://pubchem.ncbi.nlm.nih.gov/summary/summary.cgi?cid=5287969>
<http://pubchem.ncbi.nlm.nih.gov/summary/summary.cgi?cid=11338033>
<http://pubchem.ncbi.nlm.nih.gov/summary/summary.cgi?cid=5287969>
<http://pubchem.ncbi.nlm.nih.gov/summary/summary.cgi?cid=3025986>
<http://pubchem.ncbi.nlm.nih.gov/summary/summary.cgi?cid=644215>
<http://pubchem.ncbi.nlm.nih.gov/summary/summary.cgi?cid=5287969>
<http://pubchem.ncbi.nlm.nih.gov/summary/summary.cgi?cid=5287969>
<http://pubchem.ncbi.nlm.nih.gov/summary/summary.cgi?cid=59588070>
<http://pubchem.ncbi.nlm.nih.gov/summary/summary.cgi?cid=644215>
<http://pubchem.ncbi.nlm.nih.gov/summary/summary.cgi?cid=59588070>
<http://pubchem.ncbi.nlm.nih.gov/summary/summary.cgi?cid=59588070>
<http://pubchem.ncbi.nlm.nih.gov/summary/summary.cgi?cid=644215>
<http://pubchem.ncbi.nlm.nih.gov/summary/summary.cgi?cid=644215>
None
<http://pubchem.ncbi.nlm.nih.gov/summary/summary.cgi?cid=11338033>
<http://pubchem.ncbi.nlm.nih.gov/summary/summary.cgi?cid=644215>
<http://pubchem.ncbi.nlm.nih.gov/summary/summary.cgi?cid=11338033>

Cell-line

HME1
HME1
MDAMB231
HME1
MCF10A
HME1
MDAMB231
MDAMB231
HME1
BT20
HS578T
HME1
HME1
MDAMB231
MDAMB231
HME1
HME1
HS578T
HME1
HME1
HME1
MDAMB231
BT20
HME1
HME1
HME1
SKMEL1
BT20
PC3
BT20
HME1
BT20
HS578T
MDAMB231
HME1
HS578T
HS578T
HS578T
HME1
HS578T
BT20
LNCAP
MDAMB231
MDAMB231
LNCAP
HME1
HS578T
HME1

None

<http://pubchem.ncbi.nlm.nih.gov/summary/summary.cgi?cid=644215><http://pubchem.ncbi.nlm.nih.gov/summary/summary.cgi?cid=3025986>

HME1

BT20

HS578T

Dose	Time	URL
0.12um	3h	https://maayanlab.cloud/L1000CDS2/meta?sig_id=LJP006_HME1_
1.11um	3h	https://maayanlab.cloud/L1000CDS2/meta?sig_id=LJP006_HME1_
3.33um	3h	https://maayanlab.cloud/L1000CDS2/meta?sig_id=LJP006_MDAM
0.04um	3h	https://maayanlab.cloud/L1000CDS2/meta?sig_id=LJP006_HME1_
3.33um	3h	https://maayanlab.cloud/L1000CDS2/meta?sig_id=LJP006_MCF1C
10um	3h	https://maayanlab.cloud/L1000CDS2/meta?sig_id=LJP006_HME1_
0.37um	3h	https://maayanlab.cloud/L1000CDS2/meta?sig_id=LJP006_MDAM
0.04um	3h	https://maayanlab.cloud/L1000CDS2/meta?sig_id=LJP006_MDAM
10um	3h	https://maayanlab.cloud/L1000CDS2/meta?sig_id=LJP006_HME1_
0.37um	3h	https://maayanlab.cloud/L1000CDS2/meta?sig_id=LJP006_BT20_
3.33um	3h	https://maayanlab.cloud/L1000CDS2/meta?sig_id=LJP006_HS578
3.33um	3h	https://maayanlab.cloud/L1000CDS2/meta?sig_id=LJP006_HME1_
1.11um	3h	https://maayanlab.cloud/L1000CDS2/meta?sig_id=LJP006_HME1_
3.33um	3h	https://maayanlab.cloud/L1000CDS2/meta?sig_id=LJP006_MDAM
3.33um	3h	https://maayanlab.cloud/L1000CDS2/meta?sig_id=LJP005_MDAM
0.04um	3h	https://maayanlab.cloud/L1000CDS2/meta?sig_id=LJP006_HME1_
0.12um	3h	https://maayanlab.cloud/L1000CDS2/meta?sig_id=LJP006_HME1_
3.33um	3h	https://maayanlab.cloud/L1000CDS2/meta?sig_id=LJP005_HS578
0.37um	3h	https://maayanlab.cloud/L1000CDS2/meta?sig_id=LJP006_HME1_
1.11um	3h	https://maayanlab.cloud/L1000CDS2/meta?sig_id=LJP006_HME1_
1.11um	3h	https://maayanlab.cloud/L1000CDS2/meta?sig_id=LJP006_HME1_
3.33um	3h	https://maayanlab.cloud/L1000CDS2/meta?sig_id=LJP006_MDAM
0.12um	3h	https://maayanlab.cloud/L1000CDS2/meta?sig_id=LJP006_BT20_
0.12um	3h	https://maayanlab.cloud/L1000CDS2/meta?sig_id=LJP006_HME1_
10um	3h	https://maayanlab.cloud/L1000CDS2/meta?sig_id=LJP006_HME1_
0.08um	6.0h	https://maayanlab.cloud/L1000CDS2/meta?sig_id=CPC006_SKMEI
3.33um	3h	https://maayanlab.cloud/L1000CDS2/meta?sig_id=LJP006_BT20_
10.0um	6.0h	https://maayanlab.cloud/L1000CDS2/meta?sig_id=CPC009_PC3_6
3.33um	3h	https://maayanlab.cloud/L1000CDS2/meta?sig_id=LJP006_BT20_
3.33um	3h	https://maayanlab.cloud/L1000CDS2/meta?sig_id=LJP006_HME1_
3.33um	3h	https://maayanlab.cloud/L1000CDS2/meta?sig_id=LJP006_BT20_
3.33um	3h	https://maayanlab.cloud/L1000CDS2/meta?sig_id=LJP006_HS578
1.11um	3h	https://maayanlab.cloud/L1000CDS2/meta?sig_id=LJP006_MDAM
10um	3h	https://maayanlab.cloud/L1000CDS2/meta?sig_id=LJP006_HME1_
1.11um	3h	https://maayanlab.cloud/L1000CDS2/meta?sig_id=LJP006_HS578
0.37um	3h	https://maayanlab.cloud/L1000CDS2/meta?sig_id=LJP005_HS578
0.12um	3h	https://maayanlab.cloud/L1000CDS2/meta?sig_id=LJP006_HS578
10um	3h	https://maayanlab.cloud/L1000CDS2/meta?sig_id=LJP006_HME1_
0.12um	3h	https://maayanlab.cloud/L1000CDS2/meta?sig_id=LJP006_HS578
10um	3h	https://maayanlab.cloud/L1000CDS2/meta?sig_id=LJP006_BT20_
3.33um	3h	https://maayanlab.cloud/L1000CDS2/meta?sig_id=LJP006_LNCAP
0.12um	3h	https://maayanlab.cloud/L1000CDS2/meta?sig_id=LJP006_MDAM
1.11um	3h	https://maayanlab.cloud/L1000CDS2/meta?sig_id=LJP006_MDAM
1.11um	3h	https://maayanlab.cloud/L1000CDS2/meta?sig_id=LJP006_LNCAP
0.37um	3h	https://maayanlab.cloud/L1000CDS2/meta?sig_id=LJP006_HME1_
1.11um	3h	https://maayanlab.cloud/L1000CDS2/meta?sig_id=LJP006_HS578
1.11um	3h	https://maayanlab.cloud/L1000CDS2/meta?sig_id=LJP006_HME1_

3.33um	3h	https://maayanlab.cloud/L1000CDS2/meta?sig_id=LJP006_HME1_
0.37um	3h	https://maayanlab.cloud/L1000CDS2/meta?sig_id=LJP006_BT20_
0.12um	3h	https://maayanlab.cloud/L1000CDS2/meta?sig_id=LJP006_HS578

_3H:BRD-K43389698:0.12
_3H:BRD-K88573743:1.11
IB231_3H:BRD-K19220233:3.33
_3H:BRD-K87909389:0.04
IA_3H:BRD-K88573743:3.33
_3H:BRD-K99545815:10
IB231_3H:BRD-K13390322:0.37
IB231_3H:BRD-K87909389:0.04
_3H:BRD-K99749624:10
3H:BRD-K87909389:0.37
T_3H:BRD-K88573743:3.33
_3H:BRD-K87909389:3.33
_3H:BRD-K79090631:1.11
IB231_3H:BRD-K88573743:3.33
IB231_3H:BRD-K08799216:3.33
_3H:BRD-K79090631:0.04
_3H:BRD-K79090631:0.12
T_3H:BRD-A60245366:3.33
_3H:BRD-K79090631:0.37
_3H:BRD-K43389698:1.11
_3H:BRD-K87909389:1.11
IB231_3H:BRD-K79090631:3.33
3H:BRD-K87909389:0.12
_3H:BRD-K87909389:0.12
_3H:BRD-K64800655:10
L1_6H:BRD-A13122391:0.08
3H:BRD-K72414522:3.33
iH:BRD-A68009927:10.0
3H:BRD-K87909389:3.33
_3H:BRD-K13390322:3.33
3H:BRD-K43389698:3.33
T_3H:BRD-K87909389:3.33
IB231_3H:BRD-K13390322:1.11
_3H:BRD-K87909389:10
T_3H:BRD-K43389698:1.11
T_3H:BRD-K79090631:0.37
T_3H:BRD-K87909389:0.12
_3H:BRD-K19220233:10
T_3H:BRD-K79090631:0.12
3H:BRD-K19220233:10
_3H:BRD-K19220233:3.33
IB231_3H:BRD-K79090631:0.12
IB231_3H:BRD-K79090631:1.11
_3H:BRD-K88573743:1.11
_3H:BRD-K13390322:0.37
T_3H:BRD-K79090631:1.11
_3H:BRD-K13390322:1.11

_3H:BRD-K88573743:3.33

3H:BRD-K79090631:0.37

T_3H:BRD-K43389698:0.12

